



# WPI

# Solar Silicon Epitaxy by Molten Salt Electrolysis: Life Cycle Analysis and Experimental Augmentations

---

A major qualifying project report submitted to the faculty of

**Worcester Polytechnic Institute**

In partial fulfillment of the requirements for the Degree of Bachelor of Science

17 April 2022

*Submitted by*

Alex Alonzo, ChE

Peter Catalino, ECE

Andrew Charlebois, ChE

Evan Costa, ChE

Tyler Melo, ME

*Project Advisors*

Professor Stephen Bitar, ECE

Professor Adam Powell, ME

This report represents the work of five WPI undergraduate students

submitted to the faculty as evidence of completion of a degree requirement.

WPI routinely publishes these reports on the web without editorial or peer review.

# Table of Contents

<b>Table of Contents</b>	<b>2</b>
<b>Abstract</b>	<b>1</b>
<b>Acknowledgements</b>	<b>2</b>
<b>Authorship</b>	<b>3</b>
<b>Chapter 1: Introduction &amp; Background</b>	<b>5</b>
1.1 Life Cycle Analysis	5
Introduction	5
1.1.1 Raw Material Extraction	6
1.1.2 Distribution	14
1.2 Experimental Component	17
1.3 Electrical Switch	18
1.3.1 Overview of Molten Salt Electrodeposition	18
1.3.2 Pulsed Reverse Current Protocol	20
1.3.3 PRCP in Practice	21
1.3.4 Lab Scale Model	22
<b>Chapter 2: Methodology</b>	<b>26</b>
2.1 Life Cycle Analysis	26
2.1.1 Mass & Energy Balances	27
2.1.2 Raw Material Extraction and Processing	27
2.1.3 Material Processing	28
2.1.4 Solar Silicon Production	35
2.1.5 OpenLCA Modeling	35
2.2 Experimental Component	37
2.2.1 Electrolysis preparation and execution	37

2.2.2 Silicon wafer extraction and cold mounting of sample	37
2.2.3 5-step polishing procedure was followed to prepare every silicon wafer	37
2.2.4 SEM images taken on polished sample	39
2.3 Electrical Switch	39
2.3.1 Research Objectives	39
2.3.2 Lab-Scale Model	39
Component Selection	39
Circuit Construction	40
Behavior Testing and Circuit Characterization	41
<b>Chapter 3: Results and Discussion</b>	<b>43</b>
3.1 Life Cycle Analysis	43
3.1.1 Siemens Process vs Electrolysis	43
3.1.2 Comparison of electrolysis components environmental effects	46
3.1.3 Contribution Analysis	51
3.2 Experimental Component	57
3.3 Electrical Switch	60
<b>Chapter 4: Impacts</b>	<b>68</b>
4.1 Engineering Ethics	68
4.2 Societal and Global Impacts	69
4.3 Environmental Impact	69
4.4 Codes and Standards	70
4.5 Economic Factors	70
<b>Chapter 5: Conclusion</b>	<b>72</b>
5.1 Life Cycle Analysis	72
5.2 Experimental Component	72

5.3 Electrical Switch	72
<b>Chapter 6: Bibliography</b>	<b>1</b>
<b>Appendix A</b>	<b>6</b>

## Abstract

Energy demand and net-zero carbon emission goals by 2050 remain a challenging compromise. The following report supplies an overview of the relative environmental impact of solar silicon production by electrolysis as an alternative to the conventional Siemens process, as well as experimental augmentations necessary for commercialization. A life cycle assessment (LCA) using OpenLCA software was created to evaluate the raw material extraction and distribution parameters of both production processes. The LCA results showed the environmental impact from the solar silicon process was insignificant compared to the Siemens process. An electrical switch was designed to improve product purity and a silicon nitride coating was implemented to prevent oxygenated corrosion on the silicon wafer. The electrical switch was designed for currents from 0-30A, with a configurable duty cycle and frequency, and the silicon nitride ( $\text{Si}_3\text{N}_4$ ) coating showed evidence of lesser shrinking on the silicon wafer.

## **Acknowledgements**

Thank you to Professor Powell for leading and co-advising our research project. We hope the work conducted over the course of this year helps towards a more sustainable, cost efficient method for producing silicon.

Thank you to Professor Bitar, for all your time advising and mentoring us along the way. Your help greatly accelerated the development of the electrical switch.

Thank you to Aditya Moudgal (Mechanical Engineering, M.S) for leading the electrolysis experiments as well as assisting in the laboratory. Additional thanks to Mike Collins for instructing proper use of the SEM and polishing procedures.

Thank you to Mohammad Asadikiya (Materials Science and Engineering, Ph.D.) for providing insightful input during our meetings.

## Authorship

Section	Author	Edited by
Abstract	Alex Alonzo, Peter Catalino, Andrew Charlebois, Evan Costa, Tyler Melo	Alex Alonzo, Peter Catalino, Andrew Charlebois, Evan Costa, Tyler Melo
Acknowledgments	Alex Alonzo, Peter Catalino, Andrew Charlebois, Evan Costa, Tyler Melo	Alex Alonzo, Peter Catalino, Andrew Charlebois, Evan Costa, Tyler Melo
Introduction	Alex Alonzo, Peter Catalino, Andrew Charlebois, Evan Costa, Tyler Melo	Alex Alonzo, Peter Catalino, Andrew Charlebois, Evan Costa, Tyler Melo
1	Alex Alonzo, Peter Catalino, Andrew Charlebois, Evan Costa, Tyler Melo	Alex Alonzo, Peter Catalino, Andrew Charlebois, Evan Costa, Tyler Melo
1.1	Andrew Charlebois, Evan Costa, Tyler Melo	Andrew Charlebois, Evan Costa, Tyler Melo
1.2	Alex Alonzo	Alex Alonzo
1.3	Peter Catalino	Peter Catalino
2	Alex Alonzo, Peter Catalino, Andrew Charlebois, Evan Costa, Tyler Melo	Alex Alonzo, Peter Catalino, Andrew Charlebois, Evan Costa, Tyler Melo
2.1	Andrew Charlebois, Evan Costa, Tyler Melo	Andrew Charlebois, Evan Costa, Tyler Melo
2.2	Alex Alonzo	Alex Alonzo
2.3	Peter Catalino	Peter Catalino
3	Alex Alonzo, Peter Catalino, Andrew Charlebois, Evan Costa, Tyler Melo	Alex Alonzo, Peter Catalino, Andrew Charlebois, Evan Costa, Tyler Melo
3.1	Andrew Charlebois, Evan Costa, Tyler Melo	Andrew Charlebois, Evan Costa, Tyler Melo
3.2	Alex Alonzo	Alex Alonzo

3.3	Peter Catalino	Peter Catalino
4	Alex Alonzo, Peter Catalino, Andrew Charlebois, Evan Costa, Tyler Melo	Alex Alonzo, Peter Catalino, Andrew Charlebois, Evan Costa, Tyler Melo
4.1	Tyler Melo	Tyler Melo
4.2	Peter Catalino	Peter Catalino
4.3	Evan Costa	Evan Costa
4.4	Andrew Charlebois	Andrew Charlebois
4.5	Andrew Charlebois	Andrew Charlebois
5	Alex Alonzo, Peter Catalino, Andrew Charlebois, Evan Costa, Tyler Melo	Alex Alonzo, Peter Catalino, Andrew Charlebois, Evan Costa, Tyler Melo
5.1	Andrew Charlebois, Evan Costa, Tyler Melo	Andrew Charlebois, Evan Costa, Tyler Melo
5.2	Alex Alonzo	Alex Alonzo
5.3	Peter Catalino	Peter Catalino
Appendix A	Peter Catalino	Peter Catalino



## Chapter 1: Introduction & Background

### 1.1 Life Cycle Analysis

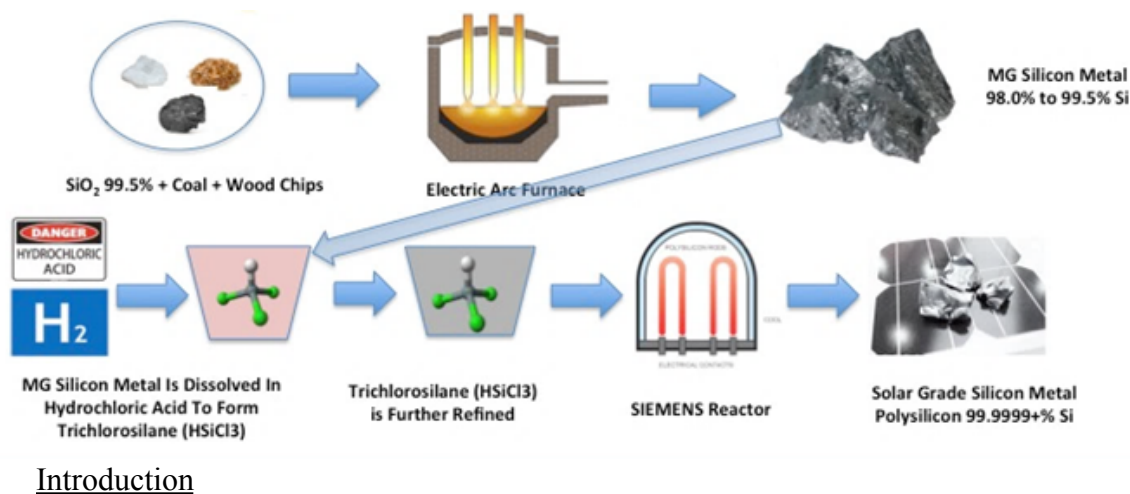


Figure 1: Timeline of  $\text{SiO}_2$  to polysilicon using Siemens Process

Across the globe, high purity polycrystalline silicon production is dominated by the Siemens Process (Jäger-Waldau, 2012). Unfortunately, this process is more akin to refinement rather than production, as it requires an already processed input which it then further refines to a purer output. More specifically, this means the process cannot accept silicon's natural form,  $\text{SiO}_2$ , as an input and relies on prior reduction from a separate process which requires its own infrastructure. In contrast, Molten Salt Electrodeposition combines these processes into one, using  $\text{SiO}_2$  as an input and directly producing high purity polycrystalline silicon as an output. Not only does this technique reduce complexity, it also promises to be safer, more cost-effective, and more environmentally friendly (Moudgal, et al., 2021). Unlike the Siemens process, which has been used to produce Silicon since the 1950's, Molten Salt Electrodeposition is new to the world of Silicon production and must first overcome a few challenges if it is to ever succeed the Siemens process as the world's predominant production method. One of these challenges is suppressing dendritic growth, a common problem for galvanostatic, constant current, electrodeposition. Dendritic growth affects the final product's purity and may also damage

production equipment in more extreme cases. Thankfully, other processes have faced similar challenges and were able to successfully prevent these divergent structures from forming with the use of a pulsed reverse current protocol, where current running through the production cell is periodically reversed. Drawing on related research, we plan to develop a pulsed reverse current protocol for Silicon electrodeposition which will be tested with a lab scale experimental model, after which we will investigate the logistics of implementing the process on an industrial scale.

### 1.1.1 Raw Material Extraction

#### **Silicon Dioxide**

Silicon dioxide ( $\text{SiO}_2$ ), commonly referred to as silica, is one of the main components required for the Solar Silicon Epitaxy process. Silica is an abundant compound found in the Earth's crust. Quartz rock is mined due to its high concentration of silica. The mined quartz is processed further to remove some impurities and separated using a gravity-based process ("How Quartz Is Processed," n.d.). The silica that enters the Solar Silicon Epitaxy process has a purity of 99.8%. According to the United States Geological Survey (USGS), the mining of silica has a limited impact on the environment except for minor disturbances in the immediate area of the worksite (Goodin, n.d.). Despite that, a large amount of energy and water is required to process the raw material.

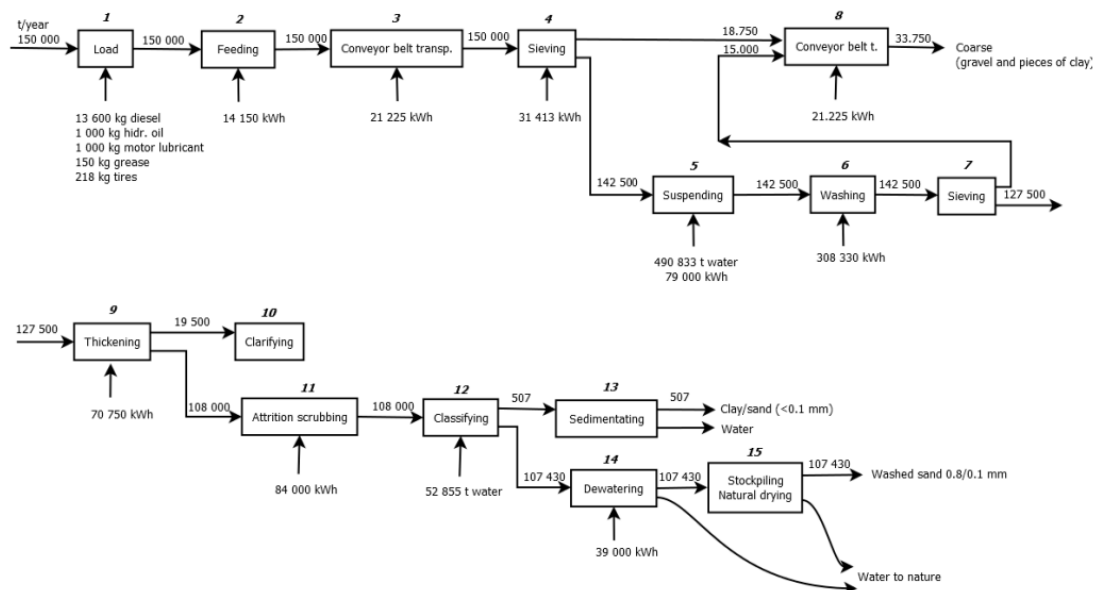
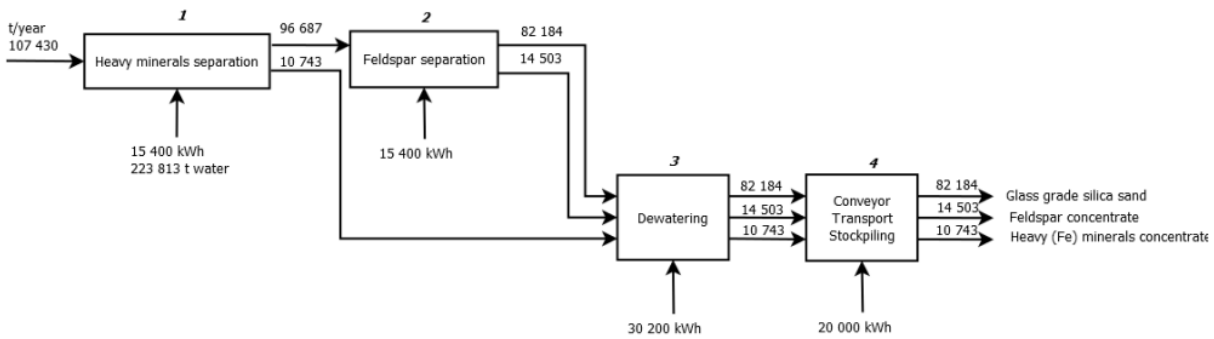


Figure 2: Process Flow Diagram of Washing and Sizing of Silica. Reprinted from “A Life Cycle Assessment of Silica Sand: Comparing the Beneficiation Processes,” by A. Grbeš, 2015, *Sustainability*, 8(1), p. 11.

Silica is usually mined using large open pits since quartz rock can be found near the surface. The pits are initially created with explosive charges to break up the hard rock layer. The loose material is then removed with bulldozers and backhoes where it is then placed into trucks to be transported to a processing facility (“How Quartz Is Processed,” n.d.). At the processing facility, the first stage involves washing and sizing the silica. Dr. Grbeš and their team at the University of Zagreb conducted a life cycle assessment(LCA) of processing silica sand. The process they assessed was producing 150 thousand tons of raw silica. An overview of washing and sizing the silica is shown in Figure 2 above. The assumptions made for the LCA were that the surface mining was done by bulldozers and trucks transporting the raw material from the mining site to the processing facility (3 km) (Grbeš, 2015). The washing and sizing of silica involve a series of different operations that all use a considerable amount of energy and water. One of the operations is sieving which separates large particles like gravel and leaves behind the finer quartz material. Next is washing which uses large amounts of water to remove surface-level and water-soluble impurities. The water is removed from the mixture and disposed of off-site and the silica is stockpiled and left to dry. The washed silica is then separated using the gravity

concentration method. A process flow diagram of the gravity concentration method is shown in Figure 2. This method takes advantage of varying densities to separate the silica from other heavy mineral contaminants. (Wills & Finch, 2016) It is assumed in the LCA that the water consumed in this operation is not recycled (Grbeš, 2015). In the end, the final product is dried glass grade silica sand.



*Figure 3: Process Flow Diagram of Gravity Concentration Method. Reprinted from “A Life Cycle Assessment of Silica Sand: Comparing the Beneficiation Processes,” by A. Grbeš, 2015, Sustainability, 8(1), p. 11.*

The LCA conducted by Dr. Grbeš analyzed 18 Midpoint impact indicators and three Endpoint impact indicators. The Midpoint indicators included equivalent CO<sub>2</sub> emissions, human toxicity, marine eutrophication, and water depletion. A few of the Endpoint indicators that were considered were human health, ecosystems, and resources. The results of the LCA found that the smallest environmental impact was attributed to the initial washing and sizing operations. Some of the cleaning processes highlighted in the process flow diagram can be omitted depending on the mined raw material purity. Removing processing steps would lead to less energy and water usage. The most significant contributors were from the machinery used, including the bulldozers and transport vehicles. The machinery uses diesel fuels and lubricating oils to maintain its operation. Endpoint impact indicators were responsible for 99.9% of human health damage, 92.5% of damage to ecosystems, and 99.9% to resource damage (Wills & Finch, 2016). Overall, they found that fossil fuel use was the most significant contributing factor to the Endpoint indicators, followed by electricity consumption and water use.

## **Salt Bath Components**

In addition to the silica, the Solar Silicon Epitaxy process requires a molten salt bath composed of  $\text{MgF}_2$  - $\text{CaF}_2$  - $\text{YF}_3$  - $\text{CaO}$ - $\text{SiO}_2$ . In the prior section, the silica component of the bath was considered. Unlike silica, the rest of the compounds required for the bath are not in their natural form. In addition to raw material extraction, processing is necessary to produce the required compounds. A production overview of each salt bath component and their subsequent environmental impact follows.

### **Magnesium Fluoride**

The first component of the salt bath is magnesium fluoride ( $\text{MgF}_2$ ). Industrially, a hydrogen fluoride source reacts with magnesium oxide to produce magnesium fluoride. Preparing magnesium oxide requires various processing steps. The raw material is extracted in the form of magnesite ( $\text{MgCO}_3$ ) (Torgal & Sánchez, 2018). Approximately 90% of magnesite is mined using open mining methods, with the other 10% conducted underground (Li et al., 2015). The magnesite then goes through basic mineral processing steps that include crushing and screening the ore to a particular size. The crushed ore is placed in reverberatory kilns and heated to a temperature between  $700^\circ\text{C}$  and  $1000^\circ\text{C}$ . This drives off the carbon dioxide from the magnesite producing light calcined magnesia or magnesium oxide ( $\text{MgO}$ ) (An & Xue, 2017). The light calcined magnesia is then cooled, screened, and ground into fine dust. A life cycle assessment was conducted for this process and focused on the environmental impact of carbon dioxide emissions. The total emissions were categorized into two groups, direct and indirect emissions. The direct emissions were from the magnesia process itself. This included the carbon dioxide released from calcination and fuel usage of the kilns (An & Xue, 2017). In China, the reverberator kilns typically use coal, heavy oil, or electricity resulting in a large amount of carbon dioxide emissions. Indirect emissions refer to energy production, whether it is coal, heavy oil, or electricity. An overview of this process is shown in Figure 4, highlighting the different types of emissions.

Industrially, fluorine is produced by electrolyzing anhydrous hydrogen fluoride that is dissolved in a bath with potassium fluoride. The electrolyzing process causes fluoride to oxidize at the anode, and hydrogen ions are reduced at the cathode (Gerberding, 2003). Anhydrous

hydrogen fluoride is prepared by distilling calcium fluoride with concentrated sulphuric acid. The reaction produces hydrogen fluoride gas which condenses and is further purified using distillation.

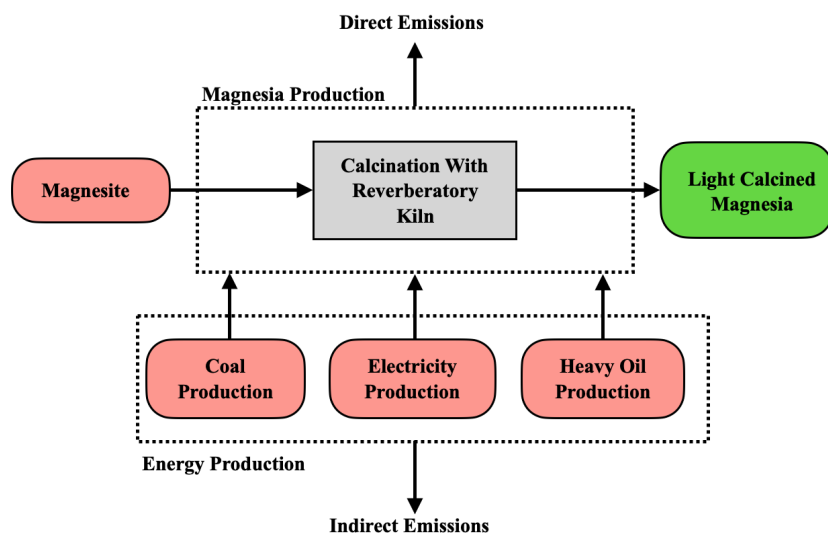
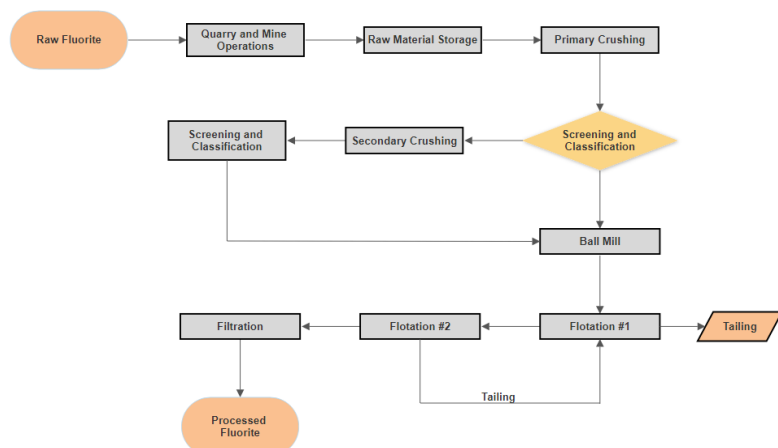


Figure 4: LCA Scope of Magnesia Production. Reprinted from “Life-cycle carbon footprint analysis of magnesia products,” by An. J., & Xue. X, 2017, *Resources, Conservation and Recycling*, 119(1), p. 4–11, <https://doi.org/10.1016/j.resconrec.2016.09.023>.

### Calcium Fluoride

The next component of the molten salt bath is calcium fluoride ( $\text{CaF}_2$ ), also referred to as fluorite. Fluorite is a colorless compound that is found naturally in the mineral fluorite (Ropp, 2013). Most fluorite mining and processing takes place in China in open-pit mines where the deposits are closer to the surface. The fluorite ore is processed using a basic mineral processing procedure that involves crushing the ore to a particular size, screening it, and separating the fluorite from impurities. Flotation is the most common method used to concentrate the fluorite and is repeated multiple times to obtain the desired purity (Zhang et al., 2018). The ore pulp enters the flotation device and is combined with water and depressants to remove the impurities. The processed material is removed from the flotation process, filtered, and dried, leading to the final product. A simplified overview of this process is shown in Figure 5.



*Figure 5: Process Flow Diagram of Calcium Fluoride Production Based on Data from EPA*

There are a variety of environmental impacts that result from fluorite manufacturing facilities. This is attributed to the basic steps of processing fluorite ore, which include: mining and beneficiation. The method used for mining fluorite is usually conducted in open pits. Open-pit mining leads to disturbances to the surrounding environment and causes particles to be released into the surrounding environment. Then there are the beneficiation processes that involve crushing, screening, and flotation. The machinery utilized in these operations typically operates on electricity. Therefore their emissions are dependent on the electrical composition of the grid. In addition, the flotation devices require water as well as depressants to sort out impurities properly. The depressants used are sodium carbonate, sodium silicate, and sodium oleate (Zhang et al., 2018). The contaminants that accumulate during the flotation steps are then moved to tailing ponds. The waste product is composed mainly of sericite and calcite minerals (Zhang et al., 2018).

### **Yttrium Oxide**

Yttrium can be found in almost all rare earth minerals and uranium ores (“Yttrium,” n.d.). The process to mine these rare earth minerals can be generalized to seven steps: mining, beneficiation, chemical treatment, separation, reduction, refining, and purifying. Yttrium is considered a heavy rare earth metal (HREE) and is mined using open-pit mines (Navarro &

Zhao, 2014). The excavated material is taken to the beneficiation process to separate the rare earth minerals from the invaluable minerals. The processing steps involved are usually a combination of grinding, gravitational separation, and froth flotation to produce a concentration of the rare earth minerals (Navarro & Zhao, 2014). Most of the environmental impact can be attributed to froth flotation since it requires a variety of chemicals to act as collectors and depressants. These chemicals, along with the impurities, eventually end up in tailing ponds that contain the waste products. The impurities can often contain heavy metals and radioactive elements, carrying a significant impact on the environment. The following beneficiation is the chemical treatment and separation of the rare earth metals. The chemical treatment is responsible for converting the rare earth minerals in the form of fluoro carbonates and phosphates to carbonates or chlorides. This process uses reagents that include inorganic acids and electrolytes. In China, it is common to use high-temperature acid roasting leading to the emission of various pollutants that include: HF, sulfur dioxide, sulfur trioxide, and silicon tetrafluoride (Navarro & Zhao, 2014). All of which have drastic impacts on the environment. The next step involves separating the yttria using liquid-liquid countercurrent solvent extractions (Britannica, n.d.).

### **Calcium Oxide**

Calcium oxide (CaO), also referred to as burnt lime, is one of the components of the molten salt bath. Calcium oxide is a product of limestone after calcination (Marinshaw et al., 1994). Limestone is a rock that is mainly calcium carbonate (CaCO<sub>3</sub>) and is mined in open quarries. The limestone is crushed and sized as it is prepared for the rotary kilns. In the kilns, the limestone is heated to high temperatures allowing for the calcination process to occur. The products that result from this procedure are calcium oxide and carbon dioxide. An example process flow diagram of calcium oxide production is shown in Figure 6 below.



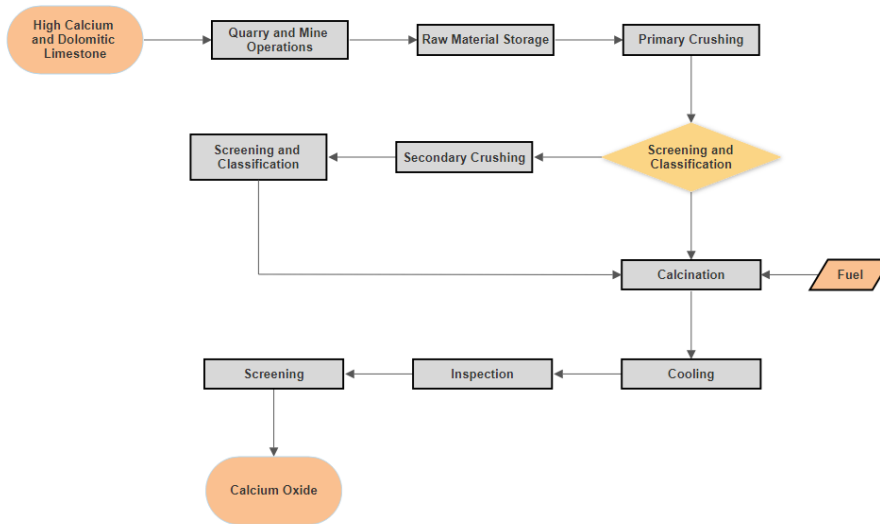


*Figure 6: Process Flow Diagram of Calcium Oxide Production Based on Data from EPA*

There are various impacts to the environment as a result of lime manufacturing plants. The most dominant pollutant is particulate matter that dissociates as the limestone is disturbed. A vast majority of these particulates arise from the rotary kilns since the rotating chamber disturbs the fine material. Some plants implement measures to control the particulates with systems like cyclone separators for larger particles and fabric and gravel bed filters for smaller particles (Marinshaw et al., 1994). In addition to particulate matter, lime production also produces a variety of gaseous pollutants that include carbon monoxide (CO), carbon dioxide (CO<sub>2</sub>), sulfur dioxide (SO<sub>2</sub>), as well as nitrogen oxides (NO<sub>x</sub>). These pollutants are byproducts of the kilns and vary based on a series of factors. Sulfur dioxide emissions are based on the fuel used for the kiln, the sulfur content in the raw feed from the mines, and the type of kiln. As a result, all of these factors can vary greatly depending on the specific conditions but can be averaged for use in an LCA. The primary sources of carbon dioxide emissions are from the calcination process of the limestone and the fuel oxidizing to heat the rotary kiln (Marinshaw et al., 1994). The EPA provides estimates for these emission factors in Table 1 based upon the type of fuel and kiln used. The factors are given in kg/Mg of lime produced.

Table 1: Emission Factors for Lime Manufacturing in kg/Mg of Lime Produced

Source	SO <sub>2</sub> <sup>b</sup>	EMISSION FACTOR RATING	SO <sub>x</sub>	EMISSION FACTOR RATING	NO <sub>x</sub>	EMISSION FACTOR RATING	CO	EMISSION FACTOR RATING	CO <sub>2</sub> <sup>c</sup>	EMISSION FACTOR RATING
Coal-fired rotary kiln (SCC 3-05-016-18)	2.7 <sup>d</sup>	D	ND		1.6 <sup>e</sup>	C	0.74 <sup>f</sup>	D	1,600 <sup>g</sup>	C
Coal-fired rotary kiln with fabric filter (SCC 3-05-016-18)	0.83 <sup>h</sup>	D	ND		ND		ND		ND	
Coal-fired rotary kiln with wet scrubber (SCC 3-05-016-18)	0.15 <sup>j</sup>	D	0.11 <sup>k</sup>	E	ND		ND		ND	
Gas-fired rotary kiln (SCC 3-05-016-19)	ND		ND		1.7 <sup>m</sup>	E	1.1 <sup>m</sup>	E	ND	
Coal- and gas-fired rotary kiln with venturi scrubber (SCC 3-05-016-20)	ND		ND		1.4 <sup>n</sup>	D	0.41 <sup>n</sup>	D	1,600 <sup>n</sup>	D
Coal- and coke-fired rotary kiln with venturi scrubber (SCC 3-05-016-21)	ND		ND		ND		ND		1,500 <sup>p</sup>	D
Coal-fired rotary preheater kiln with dry PM controls (SCC 3-05-016-22)	1.1 <sup>q</sup>	E	ND		ND		ND		ND	
Coal-fired rotary preheater kiln with multiclone, water spray, and fabric filter (SCC 3-05-016-22)	3.2 <sup>r</sup>	E	ND		ND		3.2 <sup>r</sup>	E	1,200 <sup>r</sup>	E
Gas-fired calcimatic kiln (SCC 3-05-016-05)	ND		ND		0.076 <sup>s</sup>	D	ND		1,300 <sup>s</sup>	E
Gas-fired parallel flow regenerative kiln with fabric filter (SCC 3-05-016-23)	0.0060 <sup>t</sup>	D	ND		0.12 <sup>t</sup>	D	0.23 <sup>t</sup>	D	ND	
Product cooler (SCC 3-05-016-11)	ND	ND			ND		ND		3.9 <sup>u</sup>	E

<sup>a</sup> Factors represent uncontrolled emissions unless otherwise noted. Factors are kg/Mg of lime produced unless noted. ND = no data. SCC = Source Classification Code.

<sup>b</sup> Mass balance on sulfur may yield a more representative emission factor for a specific facility.

<sup>c</sup> Mass balance on carbon may yield a more representative emission factor for a specific facility.

<sup>d</sup> References 11,20.

<sup>e</sup> References 11,13,20,31,33.

<sup>f</sup> References 20,27.

<sup>g</sup> References 10-11,26-29,31.

### 1.1.2 Distribution

When conducting a life cycle assessment on this process, an analysis on the distribution of raw material and product must be taken into account. Transportation of material through the use of air, rail, sea and truck directly contributes to carbon emissions and an accurate representation of those emissions should be analyzed within this assessment. Not only should the fuel combustion component be accounted for, but also the emissions from vehicle manufacturing, maintenance, and end of life. If only tailpipe emissions are accounted for, an underestimate of total life cycle emissions for freight transportation will be present for that of material transportation of raw materials for solar silicon epitaxy by molten salt electrolysis.

Baseline parameters for each mode of transport are provided in the table below (Cristiano Facanha and Arpad Horvath, 2007).

**TABLE 1. Input Parameters for Baseline Scenario**

variable	road	rail	air
vehicle type	model 2000 Class 8b heavy-duty diesel truck	4,000 hp diesel-electric locomotives (conforming to tier 0 standards) and 70 rail cars (double-stack) conforming to tier 0 standards	Boeing 747-400 dedicated to freight operations (conforming to 1981 standards)
equipment capacity	22.3 tons	3,721 tons	124 tons
equipment utilization	75%	75%	75%
empty miles	25%	25%	25%
average speed	50 mph	30 mph	546 mph
infrastructure	leveled four-lane asphalt highway	leveled rails and wood crossties built on top of 3 subbase layers	based on average airport

*Figure 7: Transportation Input Parameters for Baseline Scenario of road, rail, and air freight from Cristiano Facanha and Arpad Horvath, 2007, Evaluation of Life-Cycle Air Emission Factors of Freight Transportation, Environmental Science & Technology 41(20), pp. 7138-7144 doi: [10.1021/es070989q](https://doi.org/10.1021/es070989q).*

This baseline will be used as reference to estimate accurate emissions for each mode of transport involved in the movement of raw material associated with the process. Interestingly, when comparing freight trains to trucks and their associated emissions and energy, it was concluded that freight trains had three times less than trucks on a ton-mile basis (Stodolsky, 1998). Unfortunately, this study did not include transportation infrastructure within their life cycle assessment on different modes of freight travel.

It is also apparent that one mode of transportation is not to be supported more than that of other modes of transportation. First, due to most background research being based on long distance travel of 500 miles or more. Any transportation within shorter distances would not be represented accurately. Secondly, intermodal transportation considerations are not included. Lastly, not all modes of travel are in competition with one another for the same market or routes of travel.

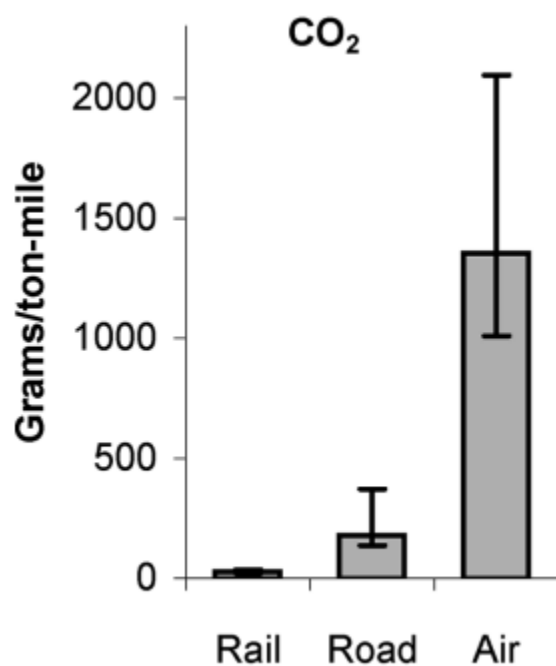


*Figure 8: Mode comparison of rail, road, and air freight from Cristiano Facanha and Arpad Horvath, 2007, Evaluation of Life-Cycle Air Emission Factors of Freight Transportation, Environmental Science & Technology 41(20), pp. 7138-7144 doi:[10.1021/es070989q](https://doi.org/10.1021/es070989q).*

Represented above in Figure 8 is a mode comparison for three main modes of freight transportation, demonstrating the grams of carbon dioxide for every ton-mile traveled. When looking directly at the emission outputs of these three main modes of transportation, it is evident that air transportation contributes the most to emissions. Rail transportation also scored better than that of road transportation for emissions by a factor of 1.2-7 (Facanha, 2007).

Vehicle type, geography and mode efficiency also play a large role in influencing emissions. First off, vehicle types have differences in fuel type as well as carrying capacities leading to variations in emission output. For example, to represent road freight travel as accurately as possible, the average size of the road vehicle should not be taken into account. The most accurate representation of road based freight travel should be the vehicle that is most

commonly used within the industry. Since most travel is longer in distance, larger vehicles are used and represent a baseline scenario for road based travel.

Secondly, geography slightly affects emissions through infrastructure maintenance, as well as rail track and road grades. Geography also plays a crucial role in air quality and health effects, more specifically among cities that have a strong presence of vehicle manufacturing plants, leading to more local emissions.

Lastly, mode efficiency plays a role in emissions through equipment utilization and share of empty miles. Improvements in equipment utilization and a reduction in backhaul directly lead to reduction in emissions. Transportation policy has not addressed these factors traditionally but private industry has been motivated to make equipment utilization improvements and reduce empty backhaul for personal economic considerations.

## **1.2 Experimental Component**

By 2050, the U.S. plans to generate zero net carbon emissions. Desperate to set an example in the battle against climate change, clean energy sources are surging in demand in the U.S., and domestic manufacturing of solar panels and wind farms are re-entering international competition. Several new innovations in clean energy are undergoing heavy research and commercialization, from fusion energy to hydrogen fuel. Meanwhile, solar and wind power offer the most reliable and abundant sources of clean energy. Economic restraints determine ultimately which clean energy technology is set to dominate the industry—and now with a much more concerning factor of environmental impact. Currently, the U.S. has targeted half of electricity sourced from solar power to meet zero net carbon emissions. Consequently, lower cost of photovoltaic systems must be met in order to fulfill this goal. Many innovations are tackling this issue from 3D printing solar cells from a single layer of powdered silicon to refinement of existing, traditional processes such as the Siemens process.. However, a promising alternative is in silicon epitaxy by molten salt electrolysis using pulse current electrodeposition.. The practice of using molten salt electrolysis for the production of silicon is not an entirely new concept. The electrochemical process operates in such a way that a combination of salts are heated in a furnace and then an electric current is passed through the molten mixture, known as a bath, from a

cathode to an anode. Multiple experimental trials have been completed for the production of silicon through molten salt electrolysis, but were not nearly pure enough for solar grade silicon, in addition to several impurities in need of separation beforehand (4). Electrolysis is carried out in an electrolytic cell, in which there are positive and negative electrodes separated by some distance and in contact with the bath solution (3). Therefore, design choices for the electrodes, bath composition, temperature, and current in electrolysis experiments are important in optimizing the purity of a solar-grade silicon product.

Generally a specific feature of metal deposition by pulse electrolysis compared with other methods of producing a metal or a compound is that we can prescribe the driving force (i.e. the free energy) of the process by applying a given potential to the electrode or we can prescribe a certain reaction rate by applying a given current (1). However, in previous experiments the solid silicon cathode shrunk during the electrolysis, granting much smaller yields of silicon product. Silicon nitride ( $\text{Si}_3\text{N}_4$ ) is a promising hard ceramic material with several excellent properties such as chemically inert, corrosion resistance, high hardness and high-temperature stability which retains its room temperature strength up to  $1200\text{ }^\circ\text{C}$  (2).

## **1.3 Electrical Switch**

### **1.3.1 Overview of Molten Salt Electrodeposition**

Before investigating the various methods to produce evenly deposited silicon, it is important to understand the fundamentals behind the overall process. Molten Salt Electrodeposition begins with heating a mixture of various salts including  $\text{CaF}_2$ ,  $\text{MgF}_2$ ,  $\text{CaO}$ ,  $\text{SiO}_2$ , and  $\text{YF}_3$  in a furnace to  $1100^\circ\text{C}$  (Moudgal, et al., 2021). Notice how this process directly makes use of silicon's natural form,  $\text{SiO}_2$ . After the salt mixture becomes molten and has reached  $1100^\circ\text{C}$ , a silicon cathode and a yttria-stabilized zirconia anode are inserted into the mixture. Once inserted, a current is passed through the electrolytic cell, initiating the deposition process.

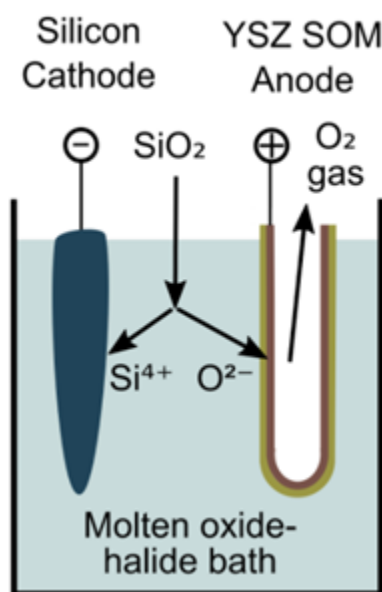


Figure 9: Illustration of Molten Salt Electrodeposition cell (Moudgal, et al., 2021).

Ideally, this process should produce a structurally homogeneous silicon deposit, free of impurities. However, previous research has suggested this outcome to be unlikely, as past experimentation resulted in impure deposits of silicon with varied morphological features (Cohen, 1977). To explain this, it may be helpful to take a deeper look at how the deposit forms. In the cell, the rate of deposition is directly proportional to the applied current's magnitude (Despic & Purenovi, 1974). Essentially, the larger the applied current, the faster material deposits. However, there are tradeoffs between the rate of deposition and the quality of the deposit. When a larger current is used, the material deposits faster and less evenly, while a smaller current produces material slower and more evenly. Even deposition is particularly important as it contributes to the deposit's purity and structure, so although material could be deposited faster at the expense of evenness, it would be less suitable for applications in solar technology. Additionally, both small and large currents are susceptible to the sporadic formation of aberrant crystal formations, or dendrites, which sprout out from the bulk deposit at random. Referred to colloquially as needle bushes, dendrites protrude out from the deposition and greatly contribute to unevenness. Nonetheless, if Molten Salt Electrodeposition is ever to be used as a viable means of silicon production, preventative measures should be investigated to suppress these abnormalities and ensure evenness.

### 1.3.2 Pulsed Reverse Current Protocol

Preventing undesirable surface morphology on electrodeposited material is not a challenge unique to silicon, as other industries have already faced and solved similar production issues (Popov, Maksimović, Zečević, & Stojić, 1986). Utilizing either chemical additives or current waveforms, these industries were able to consistently produce electrodeposited material free of surface aberrations. In this section, we explore how an oscillating current waveform could be used to prevent surface aberrations in electrodeposited silicon.

Galvanostatic, or constant current, electrodeposition is especially prone to dendrites, as current is continuously applied, allowing for unimpeded growth (Cohen, 1977). While unimpeded growth may sound attractive in terms of output, it is applicable to both the bulk deposit as well as the dendritic formations. Essentially, when dendrites are formed under these conditions, they continue growing, as there is no mechanism in place to reverse this undesirable growth. However, if current is reversed across the electrodes, the dendrites can be dissolved, as the deposition process is reversed as well (United States of America Patent No. 61/174,395, 2013). A pulsed reverse current protocol seeks to make use of both modes of operation, depositing material efficiently while also periodically dissolving aberrant growth. To compare the deposition to painting a surface, numerous thin coats create a much more even finish than a single thick coat (Moudgal, Informal Overview of Molten Salt Electrodeposition Mechanics, 2021). Further, a single thick coat is at much larger risk of developing imperfections such as drips, or dendrites in the case of electrodeposition.

A Pulsed Reverse Current Protocol (PRCP) may be used to combat dendritic formations and promote evenness across deposited material. In the context of electrodeposition, A PRCP consists of a cathodic pulse for a specific duration followed by an

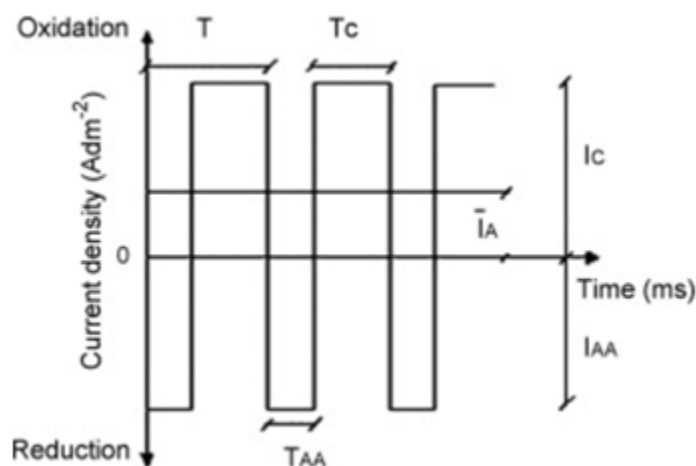




*Figure 10: PRCP waveform.  $I_c$  is cathode current,  $I_{aa}$  is anode current.  $T$  is period of waveform,  $T_c$  is time of cathode pulse,  $T_{aa}$  is time of anode pulse (Chandrasekar & Pushpavanam, 2008).*

anodic pulse for another specific duration. Generally, the cathodic pulse's duration is longer than the anodic, to deposit material most efficiently. Starting with the cathodic pulse, the targeted material is deposited onto the Cathode, after which a shorter anodic pulse occurs, which dissolves the most recent layer of deposition and expels trapped impurities from the deposit. In this way, the technique circumvents the possibility of anomalous crystal growth by depositing material intermittently with rectification cycles between each period of growth. For example, if a dendrite were to form during one of these cycles, it would not be able to grow very large and the period of reverse current would dissolve it as well as clean the deposit's surface before adding a new layer. This effect solves the challenge of dendritic growth, while also providing the added benefit of additional purification throughout the process.

### 1.3.3 PRCP in Practice

Conceptually, pulsed reverse current protocols seem like an elegant solution to silicon electrodeposition's largest roadblock, but theory and practice do not always align. With that in mind, it becomes imperative to examine existing research for proof of this practice's application in silicon production.

One particularly relevant study investigated the properties and appearance of silicon electrodeposited with and without a PRCP in place, albeit using different electrodes and salt mixture. Nonetheless, they found that adopting a PRCP completely prevented the formation of dendrites, and even allowed even deposition to occur at higher current densities (Cohen, 1977).

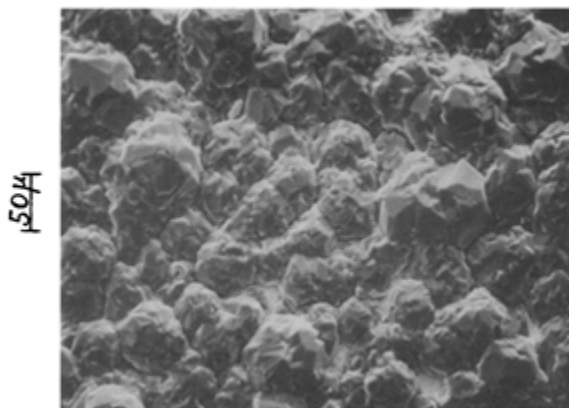


*Figure 11: Surface topography of silicon deposited with a PRCP @ 4 mA/cm<sup>2</sup> (Cohen, 1977)*

Looking at **Figure 11 & 12**, we can see that the topography of the two deposits varies significantly. In **Figure 12**, we can see how the galvanostatic deposition produces a relatively even surface but is still susceptible to dendritic formations. In **Figure 11**, we can see how even at higher current density a PRPC still produces a much more uniform surface, free of aberrations.

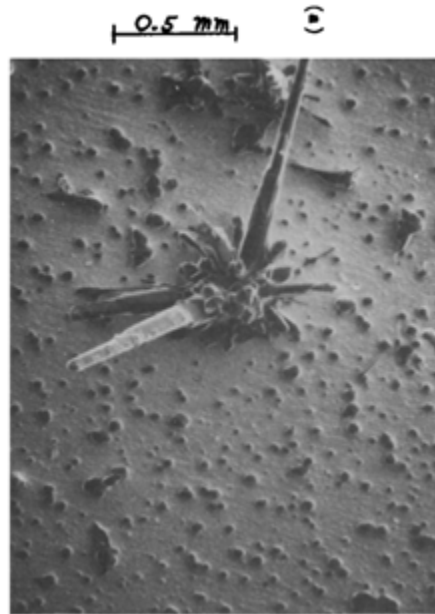


*Figure 12: Surface topography of silicon deposited galvanostatically @ 2 mA/cm<sup>2</sup> without a PRCP (Cohen, 1977).*

#### 1.3.4 Lab Scale Model

With previous research suggesting that a pulsed reverse current protocol effectively suppresses undesirable deposit morphology, this section explores a lab scale implementation of PRPC in molten salt electrodeposition. Specifically, we are looking to create a pulse wave rectifier which produces an square output waveform with a peak current range of 0-30A , a voltage range of 0.1-5 V, a switching frequency of 1kHz, and a 30:1 ratio of forward to reverse current (United States of America Patent No. 61/174,395, 2013) (United States of America Patent No. 849,881, 1977).

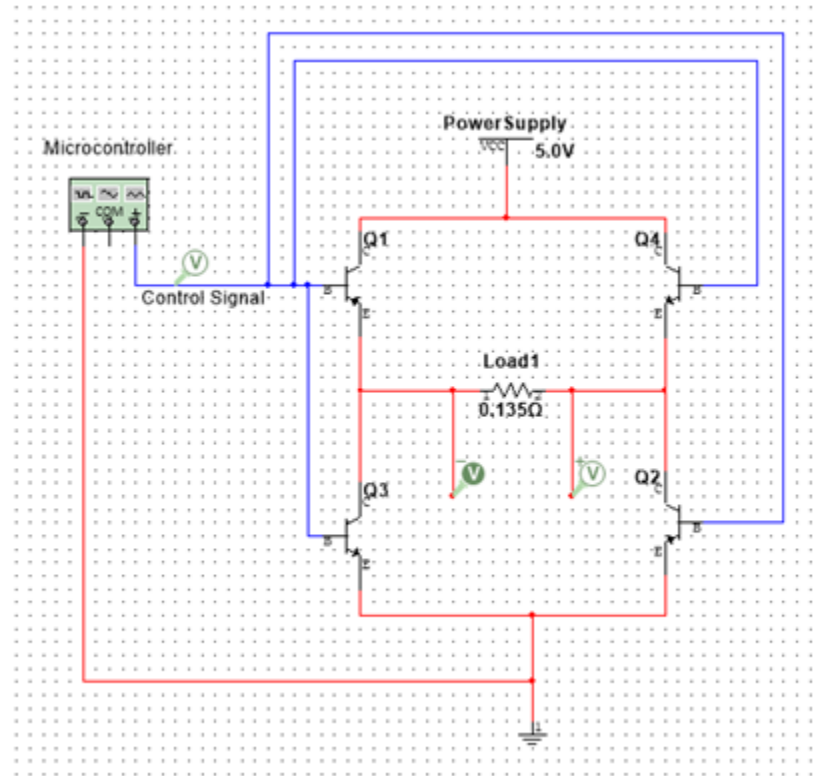


*Figure 13: Conceptual model of pulse wave rectifier*

**Figure 13** displays a conceptual model of the prototype pulse wave rectifier constructed with both NPN and PNP Bipolar Junction Transistors operated in their saturation regions. In order to periodically reverse power flow across the Load, the design utilizes four electronically controlled switches which simultaneously open and close in pairs of two, opening a path for power across the load in the desired direction and closing the alternate path. Conveniently, both pairs can operate from an identical control signal, as one pair activates with a high input signal, while the other activates with a low input signal. For example, when the control signal is high, switches Q3 and Q4 will activate allowing power to flow across the load in the forward direction. Then, when the control signal becomes low, switches Q3 and Q4 will become inactive and Q1 and Q2 will activate, allowing power to flow in reverse across the load. This behavior is illustrated in **Figures 14 & 15**.

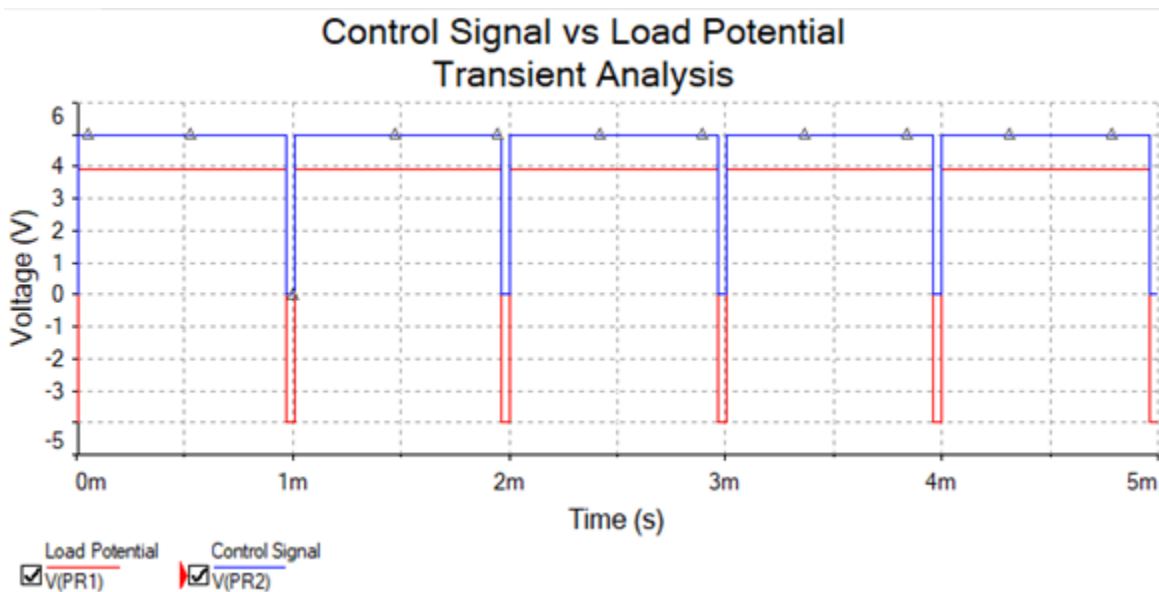


Figure 14: Simulated output of Circuit shown in Figure 6. Control signal is 5Vpk @ 1kHz with a 30:1 or ~96% Duty Cycle.

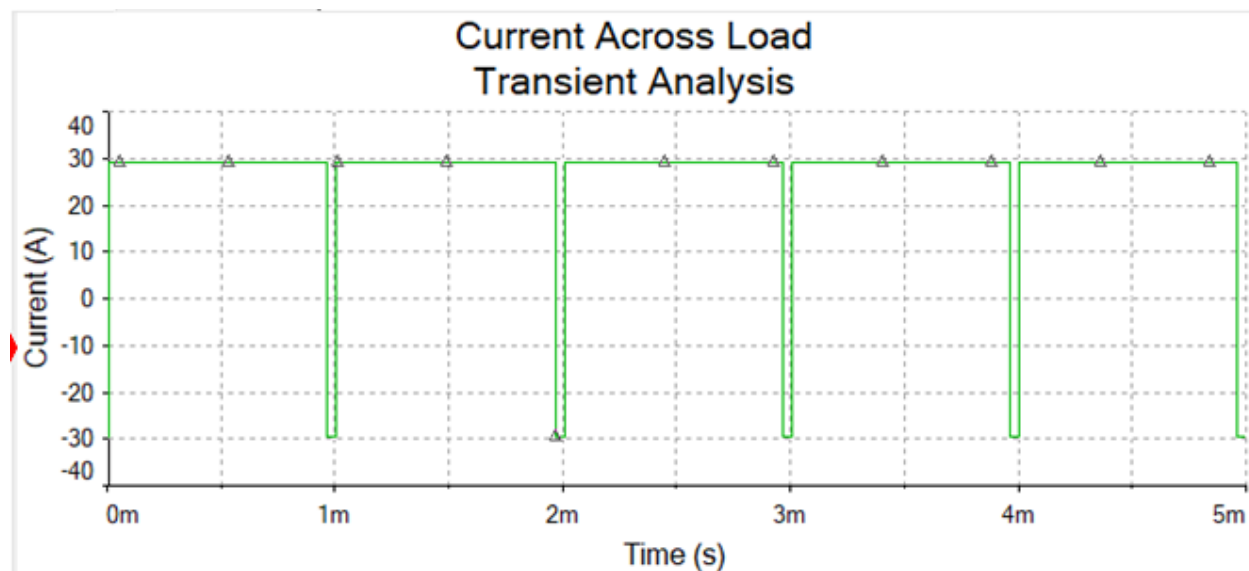


Figure 15: Simulated output of Circuit shown in Figure 6

Figure 15: demonstrates the relationship between the control signal and cell potential, when the control signal is high the cell potential is positive, when the control signal is low the cell

*potential is negative. Similarly, **Figure 15** illustrates the response of current across the load, which mirrors the cell's potential in direction and duration.*

Simulation data appears to support **Figure 13**'s ability to produce the desired power responses across the load. While these results do provide a proof of concept, specific components must still be selected for the construction of a physical circuit. Part Selection will be focused on in the methodology and possible component alternatives are Bipolar Junction Transistors (BJTs), Metal Oxide Semiconductor Field Effect Transistors (MOSFETs) as well as prefabricated Integrated Circuits with analogous behavior.

## Chapter 2: Methodology

### 2.1 Life Cycle Analysis

When testing a new process, it is necessary, given the increased awareness of the importance of environmental protections, to understand the possible impacts associated with the system. This is why a life cycle analysis is so useful as it allows for just this to be done. In order to conduct a life cycle analysis however, it is first necessary to consult the International Organization for Standards, or ISO, in order to follow their guidelines. For this life cycle analysis, two standards were examined, *Life Cycle Assessment - Requirements and Guidelines*, and *Life cycle Assessment - Principles and Framework*.

#### 1. Requirements and Guidelines

The ISO standards titled requirements and guidelines predictably give the guidelines for conducting a life cycle analysis. The first general requirement is that the LCA should include the goal and the scope of the process. This is so that it is known what is being accomplished by the process, and how in depth the analysis of this process goes, i.e are there any components of the process not included in the LCA for some reason. There is a long list of guidelines to consider in the ISO Standards when creating the scope for the LCA as well including but not limited to: The function of the product system, the system boundary, assumptions made, and limitations.

There needs to also be an inventory analysis of the components being used so that their impact can be further understood. For this section, there should be flow diagrams created that outline all the unit processes that are modeled as well as their interrelationships. This should also include a description of the data collection and calculation methods used as well as a list that specifies the units being used. The final requirement for an LCA is an impact assessment and interpretation of results. This must include analysis of the quality of the impact data and results to see if it aligns with the scope and goals of the project. (*International Organization for Standards [ISO] 14044, 2006*)

#### 2. Principles and Framework

The principles and frameworks ISO standards go into more specific detail into parts of the Life Cycle Analysis, however generally states nearly if not completely identical information. Some extra details it gives about the goal of an LCA is that it must state: the intended application, the reasons for carrying out the study, the intended audience, and whether the results are meant to be comparative to another process or not. (ISO, 2006)

### 2.1.1 Mass & Energy Balances

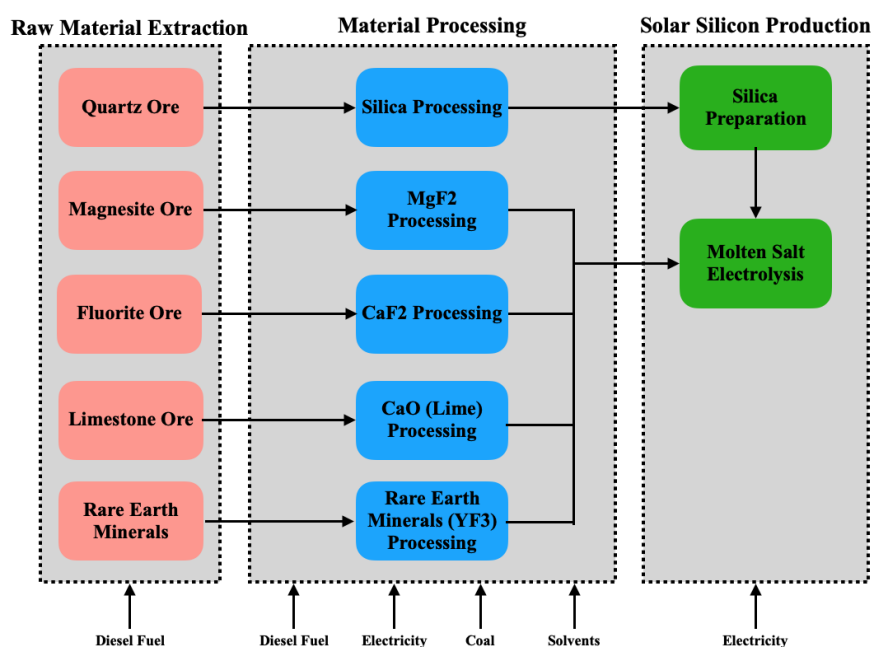


*Figure 16: Overview Process Flow Diagram of Life Cycle Assessment*

### 2.1.2 Raw Material Extraction and Processing

The raw materials required for solar silicon production include quartz, magnesite, fluorite, limestone, and rare earth minerals. A mass balance will be conducted to attribute the emissions associated to the extraction of each raw material. This mass balance will be built upon one conducted by Aditya and a prior MQP team for the Solar Silicon Production process. The mass balance was extended to include both the raw material extraction and material processing with the given amounts of each input to produce 1kg of solar silicon. Knowing the mass of the

material going through each process outlined in Figure 16 will indicate the emissions attributed to each step. When it comes to raw material extraction, the minerals are typically mined using an open-pit method with the help of bulldozers and backhoes to break up and collect loose material. These vehicles operate on diesel fuel which as a result produces carbon dioxide emissions. The Environmental Footprint V2.0 database that is included with OpenLCA provides system processes for the production of materials. The scope of these processes includes the extraction of the raw materials and the emissions are weighted based on the quantity of the final product.

### 2.1.3 Material Processing

Following the extraction of minerals from the mines, they all go through some level of mineral processing to produce a highly concentrated final product. For the life cycle assessment, it is assumed that the processing of these materials occurs on-site alongside the raw material extraction. The transportation involved in moving the material on-site is included in the processes provided by the Environmental Footprint database. The material processing section outlined in Figure 16 includes the steps required to convert the raw material ores to their intermediate products. These then become the inputs to the solar silicon production process.

#### Silicon Dioxide

The preparation of silicon dioxide, also referred to as silica, includes a series of basic mineral processing steps followed by separation to produce high concentration silica. The basic mineral processing steps include washing and sizing the silica as shown in detail in Figure 2. The washed silica is then further purified using the gravity concentration method as indicated in Figure 2. The figures are from a life cycle assessment conducted by Dr. Grbeš and his team, who performed a case study on a plant in Croatia that produces 150,000 tons of silica annually. A general system view of this process is shown in Figure 17 below. From the process flow diagram, it is evident how much electricity and diesel is consumed to produce 82,184 tons of silica per year. This contributes to about 8.87 KWh per ton of silica and 0.165 kg of diesel per ton of silica. These values were compared to the system process outlined in the Environmental Footprint V2.0 database which was facilitated by the European Commission. The values were similar but the process from the database was more comprehensive and accounted for multiple environmental impact factors. The process was based upon the industry standard in Europe which involved the



mining of quartz followed by cleaning, grinding, screening and separation to produce silica sand. The amount of silica sand product was based upon the mass balance conducted by the prior MQP to determine the environmental impact of the process. The emissions related to electricity consumption was based upon Europe's average electricity supply composition. It was decided to source the silica from the plant in Croatia to match the assumptions made by the database that were based on the industry in Europe.

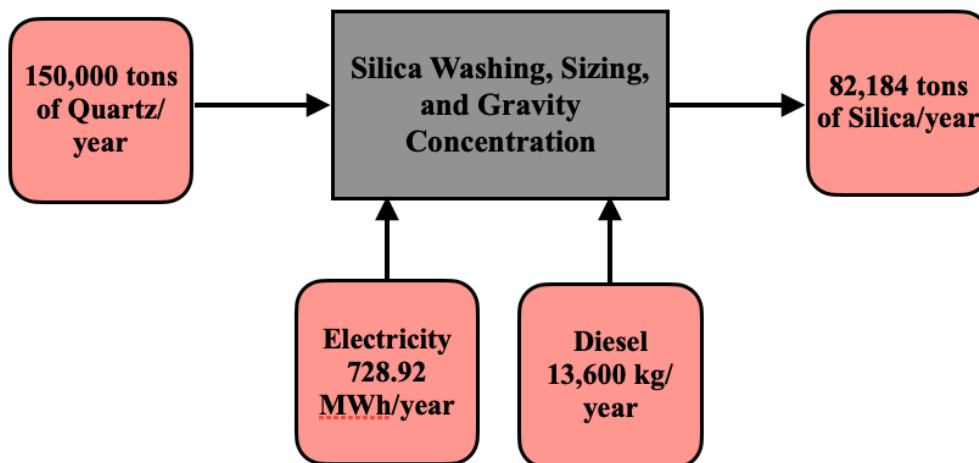


*Figure 17: System Level Inputs & Outputs of Washing, Sizing, & Gravity Concentration Method. Reprinted from "A Life Cycle Assessment of Silica Sand: Comparing the Beneficiation Processes," by A. Grbeš, 2015, Sustainability, 8(1), p. 11.*

### Magnesium Fluoride

The preparation of magnesium fluoride is industrially conducted by reacting a hydrogen fluoride source with magnesium oxide (MgO). Magnesium oxide is a product of magnesite ore (MgCO<sub>3</sub>) using the process of calcination. The magnesite ore first goes through a series of basic mineral processing steps which includes crushing and screening the ore to a particular size. The processed ore is fed into reverberatory kilns and heated to a temperature between 700°C and 1000°C. The kilns drive off carbon dioxide contributing to the total emissions from this process. The output is cooled, screened, and ground into fine dust leading to the final product of magnesium oxide. The Environmental Footprint database includes a magnesium oxide production process that starts with the mining of magnesite ore and ends with the caustic magnesium oxide (MgO). This assessment includes the calcination process as well as the

preliminary basic processing steps like crushing and screening the ore. The assessment accounted for both direct and indirect emissions. The direct emissions were from the magnesia process itself. This included the carbon dioxide released from calcination and fuel usage of the rotary kilns (An & Xue, 2017). It was decided to source the magnesium oxide from Martin Marietta which operates a plant in Michigan, US. The indirect emissions refer to energy production, whether it is coal, heavy oil, or electricity. Since the database is primarily focused on European industry, the electricity emissions are based upon the electricity supply composition of Europe. The process from the database is self contained and there is no clear way to modify the electricity supply composition therefore there will be some discrepancy. The magnesium oxide is then reacted with a hydrogen fluoride source to produce magnesium fluoride. In industry, the common reaction is the following:  $\text{MgO} + (\text{NH}_4)\text{HF}_2 \rightarrow \text{MgF}_2 + \text{NH}_3 + \text{H}_2\text{O}$ . The only process within the Environmental Footprint database that produces a fluoride source is the production of HF. Researching providers, it was decided that the HF was sourced from Honeywell HF facility in Bryan, TX. It is assumed that the combination of MgO and HF is a viable process to make  $\text{MgF}_2$ . The reaction was balanced to determine the quantity of MgO and HF given the amount of  $\text{MgF}_2$  from the mass balance from the previous MQP. The process of producing  $\text{MgF}_2$  is not well documented to recreate in OpenLCA and there are no pre-existing LCAs within the open source databases. Therefore, a dummy process was inserted as a place-holder to act as a recipient for the two reactants. However, there are no impacts related to the  $\text{MgF}_2$  process itself. Oakwood Products, Inc is a prominent magnesium fluoride producer located in Estill, SC.

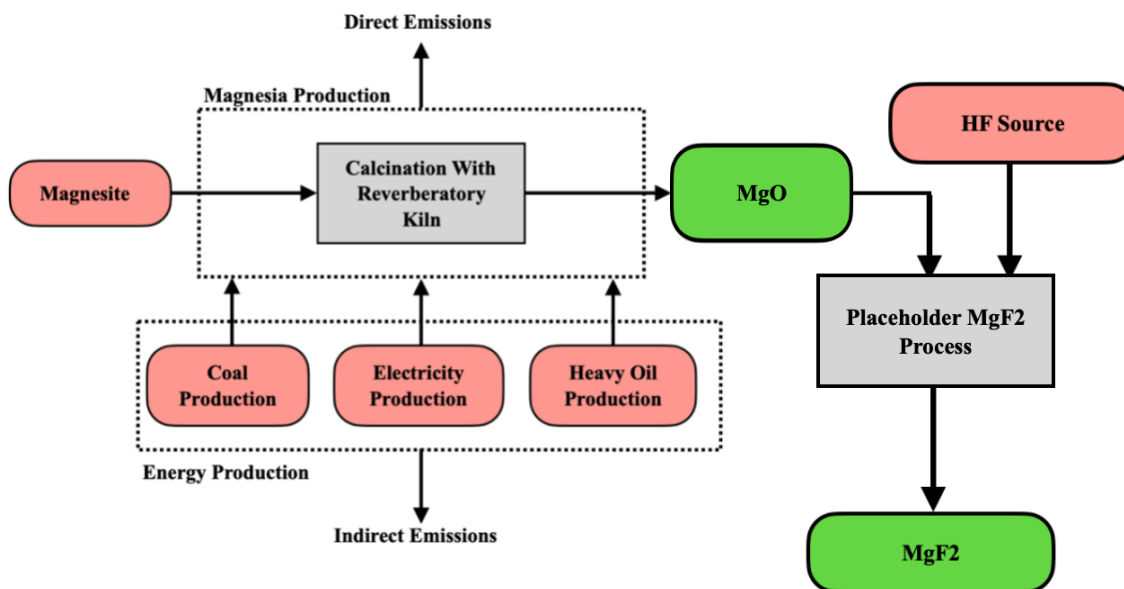


Figure 18: LCA Scope of Magnesium Fluoride Production. Reprinted from “Life-cycle carbon footprint analysis of magnesia products,” by An. J., & Xue. X, 2017, *Resources, Conservation and Recycling*, 119(1), p. 4–11, <https://doi.org/10.1016/j.resconrec.2016.09.023>.

### Calcium Fluoride

The preparation of calcium fluoride ( $\text{CaF}_2$ ), also referred to as fluorite, begins with the fluorite mineral ore. The ore is first processed using a series of mineral processing steps that involve crushing the ore to a particular size, screening it, and separating the fluorite from impurities. The preferred method for separation is flotation and is repeated multiple times to obtain the desired purity (Zhang et al., 2018). A detailed overview of the various process steps are included in the background section and illustrated in Figure 16. A life cycle assessment of this process has been conducted and the system process is included in the Environmental Footprint V2.0 database. The scope of the process includes the mining of the fluorite, crushing the ore, screening it, and washing it to produce calcium fluoride. The quantity of  $\text{CaF}_2$  required was based upon the mass balance from the previous MQP. The theoretical plant was positioned at the Blanchard Mine in New Mexico, US. The electricity mix modeled by the process uses the global average for the supply composition of electricity. Ideally, this would be changed to the US

average or more specifically New Mexico. However, the parameters necessary to modify the electricity mix are not adjustable. Despite that, the process still provides a good idea as to the environmental impacts associated with the preparation of calcium fluoride.

### Yttrium Oxide

Yttrium oxide ( $Y_2O_3$ ), also referred to as yttria, is a compound that is found in almost all rare earth minerals and uranium ores (“Yttrium,” n.d.). Therefore, the processing steps for yttrium oxide is synonymous to that of other rare earth metals. A life cycle assessment was conducted for the processing of rare earth metals which considered various rare earth oxides. The scope of the life cycle assessment is shown in Figure 19. The processing steps involved are usually a combination of grinding, gravitational separation, and froth flotation to produce a concentration of the rare earth minerals (Navarro & Zhao, 2014). Froth flotation is most commonly used since it is very effective but has extra inputs that involve chemicals to act as collectors and depressants. The processed ore then gets chemically treated with the introduction of reagents that include inorganic acids and electrolytes. In China, typical practice is to use high-temperature acid roasting leading to the emission of various pollutants that include: HF, sulfur dioxide, sulfur trioxide, and silicon tetrafluoride (Navarro & Zhao, 2014). The Environmental Footprint V2.0 database provides a system process for the production of rare earth concentrate based on the industry standard in China. It also models the electricity mix to be consistent with China’s average electricity supply composition. The specific facility that was chosen was Bayan Obo Mine in the Bayan Obo Mining District in China. The process outlined includes the mining of the ore, crushing it, concentrating it using magnetic separation and flotation producing the rare earth concentrate. This product is a collection of rare earth oxides therefore the emissions attributed to yttrium oxide were based upon its market value. As of conducting the life cycle assessment, yttrium oxide has a value fraction of 1-1.5% (Koltun & Tharumarajah, 2010). Within OpenLCA, the adjustment was made by creating a parameter that multiplies the amount of yttrium oxide required from the mass balance by 1.2%. This weights the bulk emissions from the rare earth process so it only reflects that of the preparation of yttrium oxide.

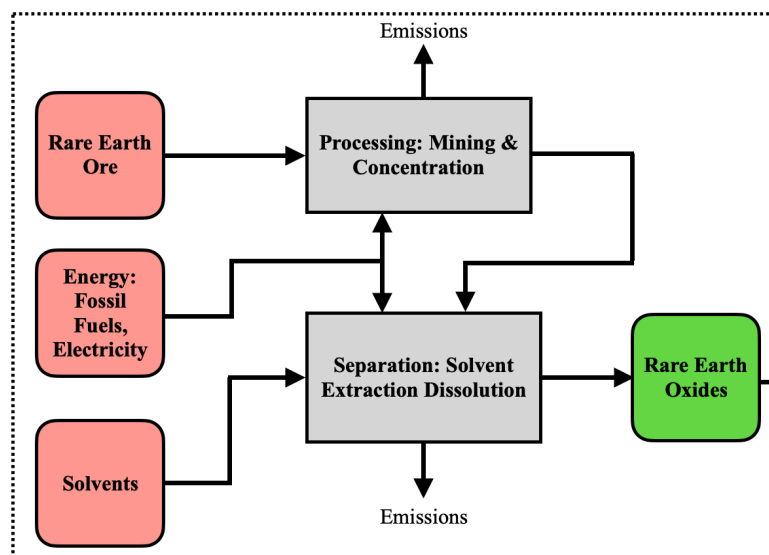


Figure 19: LCA Scope of Rare Earth Oxide Production from Ecoinvent Database Outlined by Dotted Line with Inclusion of Fluoride to Produce  $YF_3$  (Althaus et al., 2007).

### Calcium Oxide

The preparation of calcium oxide (CaO), also referred to as burnt lime, is the result of exposing limestone to high temperatures through calcination. Limestone is a rock that is composed mainly of calcium carbonate ( $CaCO_3$ ). The limestone first goes through basic processing steps that include crushing and sizing the stone to prepare it for the rotary kilns. In the kilns, the limestone is heated to high temperatures allowing for the calcination process to occur. The products that result from this procedure are calcium oxide and carbon dioxide. A general system view of this process is shown in Figure 20 below that highlights the inputs and outputs. Lime production produces a variety of gaseous pollutants that include carbon monoxide (CO), carbon dioxide ( $CO_2$ ), sulfur dioxide ( $SO_2$ ), as well as nitrogen oxides (NOX). These pollutants are byproducts of the kilns and vary based on a series of factors. Sulfur dioxide emissions are based on the fuel used for the kiln, the sulfur content in the raw feed from the mines, and the type of kiln. As a result, all of these factors can vary greatly depending on the specific conditions but can be averaged for use in an LCA. The primary sources of carbon dioxide emissions are from the calcination process of the limestone and the fuel oxidizing to heat the rotary kiln (Marinshaw et al., 1994). The Environmental Footprint V2.0 database includes a system process for the

cradle to gate preparation of lime which is based on the industry standard in Germany. This however means that the electricity mix is also representative of Germany's electricity supply. The theoretical plant to source the calcium oxide was located in Annville, PA by Carmeuse Lime & Stone. Ideally, this would be adjusted to the US average mix or more specifically Pennsylvania. However, similar to the other processes, the parameters necessary to modify the electricity mix are not adjustable. Despite that, the process still provides a good idea as to the environmental impacts associated with the preparation of calcium oxide. The scope of the process includes the mining of the limestone which is then introduced into a vertical-shaft coke furnace to burn off the  $\text{CO}_2$  to produce quicklime. The quicklime is cooled and then milled to a particular size producing the final product of finelime. The mass balance from the previous MQP provides the amount of calcium oxide that is necessary for the bath to produce 1kg of solar grade silicon. With the total amount required for the input, OpenLCA can be used to determine the emissions contributed from the preparation of calcium oxide.

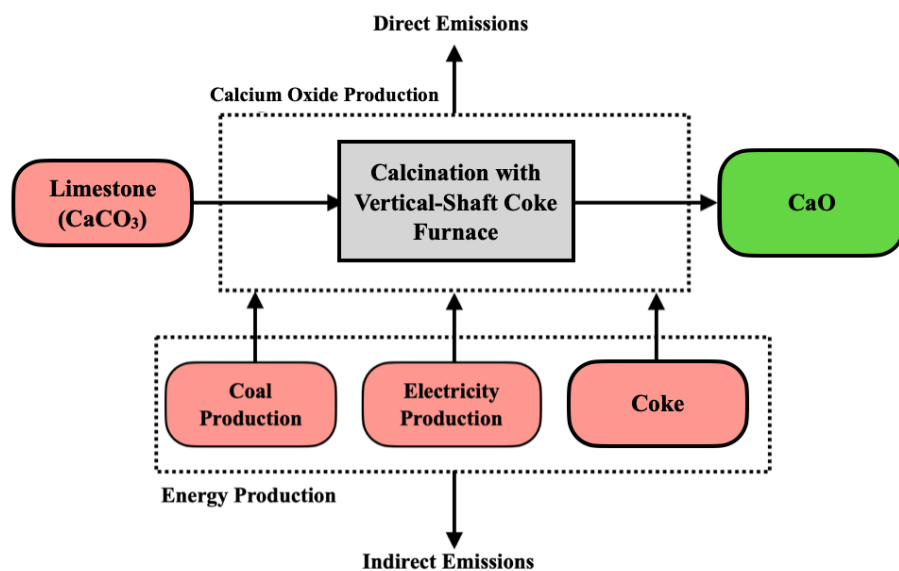


Figure 20: System Level Inputs & Outputs of the Preparation of Burnt Lime.

#### 2.1.4 Solar Silicon Production

The mass and energy balance for the solar silicon production process was completed by a prior MQP team with the help of Aditya. The mass balance breaks down the various input streams and quantifies the proposed quantities for each of them. The inputs include the silicon dioxide (the source of silicon for the process) and the molten salt bath components which are the following:  $MgF_2$ ,  $CaF_2$ ,  $Y_2O_3$ , and  $CaO$ . An energy balance was also completed and determined the amount of electricity required to produce 1 ton of solar silicon product. The emissions related to the electricity consumption will be based upon the location of the solar silicon processing plant and the region's electricity production composition. The emission factors for electricity usage for various regions of the US can be found from the EPA to determine the  $CO_2$  equivalent (EPA, 2021). The mass and energy balance will have to be extended to encompass both the material processing and raw material extraction as outlined in Fig. 14.

#### 2.1.5 OpenLCA Modeling

##### Scope of Model

As discussed previously, the life cycle assessment will focus around the raw material extraction, transportation, and manufacturing of the process being analyzed. On top of this, the use of LCIA methods within OpenLCA will be utilized. This method allows the life cycle analysis to include up to 19 environmental impact categories. These impact categories are acidification, climate change, climate change- biogenic, climate change- fossil, climate change- land use and land use change, ecotoxicity- freshwater, eutrophication- marine, eutrophication- freshwater, eutrophication- terrestrial, human toxicity- cancer, human toxicity- non-cancer, ionizing radiation- human health, land use, ozone depletion, particulate matter, photochemical ozone formation- human health, resource use- fossils, resource use- minerals and metals, and water use.

First accounting for raw materials. Materials such as silicon dioxide, magnesium fluoride, calcium fluoride, yttrium fluoride, and calcium oxide present in the molten salt bath require refining processes before use in the manufacturing of silicon. The emissions from these prior

refining processes will be taken into account using the appropriate databases within OpenLCA as well as supplementary resources from prior life cycle assessments.

Secondly, the transportation of these refined materials to the plant location. Since some of these materials are being imported overseas and traveling far distances by freight, transportation emissions will also be taken into account while conducting this life cycle assessment. OpenLCA nexus has databases for various forms of transportation emission factors.

Thirdly, the manufacturing of silicon. The process for producing solar silicon using molten salt electrolysis requires a large amount of electricity. Due to this high electrical input, we must take it into consideration within our life cycle assessment. Based upon the location of the proposed plant, the electricity being provided can vary in emission factors. For example, the higher use of fossil fuels for electricity in one area can lead to higher emission factors than that of an area with higher use of renewable energy for electricity.

#### Database Compiling

For database compiling OpenLCA nexus will be used. OpenLCA nexus data sets share a common basis of elementary flows and other reference data. As stated by OpenLCA itself, these data sets have been “mildly harmonized” in coordination with OpenLCA data providers such as PE International (GaBi databases), the ecoinvent centre (ecoinvent), or the Joint Research Centre from the European Commission (ELCD). Because of this, OpenLCA can overcome methodological differences and allow multiple databases to be combined into one database. On top of this, a comprehensive set of Life Cycle Impact Assessment methods are available and fit with reference data obtained from OpenLCA.

The environmental impact will be calculated using the ISO 14040 procedure. Included in following this procedure, the appropriate LCIA methods will be used for each database in order to remain compliant with one another. If the method does not use the same flows as the processes in a database, the calculated impacts will be 0.



## **2.2 Experimental Component**

### **2.2.1 Electrolysis preparation and execution**

The salt bath composition and  $\text{SiO}_2$  was mixed in its raw form to 500g, stirred and placed inside the crucible of a batch reactor. Temperatures reached upwards of 1100 Degrees Celsius and Argon gas was run through to flush out  $\text{O}_2$  seeping in from the outside of the reactor. Temperature was maintained between 1100 and 1110 Degrees Celsius, and electrical current was passed through to begin electrolysis. Silicon was extracted and wafer samples were collected after a day.








### **2.2.2 Silicon wafer extraction and cold mounting of sample**

After electrolysis, the silicon wafer was retrieved to prepare for the sample analysis. // The silicon wafer was weak enough to break into smaller pieces. Wafers were manually broken and fitted inside the 1.5 inch diameter mold. Manually breaking the wafers prevented the need to use the Precision Saw.

The sectioned sample was casted in EpoxiCure 2, created by mixing the Epoxy Resin to Epoxy Hardener in a 4 to 1 ratio. A releasing agent was coated on all surfaces within the mold. The sample was stood up vertically within the mold using a fixation clip. The epoxy was then poured in while maintaining the position of the sample. A vacuum system was incorporated to extract all air pockets out of the resin. The samples were left in the vacuum for approximately an hour.

### **2.2.3 5-step polishing procedure was followed to prepare every silicon wafer**

A 5-step polishing procedure was followed to prepare every silicon wafer (Figure 23).

Sectioning	Precision Saw with blade recommended for microelectronic devices				
Mounting	Castable, typically EpoThin				
Surface	Abrasive / Size	Load - lbs [N] / Specimen	Base Speed [rpm]	Relative Rotation	Time [min:sec]
CarbiMet	600 [P1200] grit SiC water cooled	3 [13]	100		Until Plane
VerduTex	6µm MetaDi Supreme Diamond*	5 [22]	100		3:00
VerduTex	3µm MetaDi Supreme Diamond*	5 [22]	100		3:00
VerduTex	1µm MetaDi Supreme Diamond*	5 [22]	100		3:00
ChemoMet	0.06µm MasterMet Colloidal Silica	2 [9]	100		2:00
 - Platen  - Specimen Holder *Plus MetaDi Fluid Extender as desired					
Imaging & Analysis	Measurement & Analysis Applications, Manual Interactive Thickness				
Hardness Testing	N/A				

*Figure 21: 5-step procedure for preparing solar-grade silicon*

Once the sample was sufficiently mounted, the samples were removed from the mold and polishing took place. Using the Buehler polisher equipment, the “5stepSilicon” was selected for the procedure on the display screen, automatically changing the load weight, base speed, and timer on the equipment accordingly. The CarbiMet surface was used with water as the abrasive. All equipment was cleaned after each exchange with a polishing surface. Each sample was rinsed and dried before viewing under a microscope to keep track of polishing progress. All suspensions used underwent proper chemical waste disposal. The VerduTex surface with 6µm diamond suspension was used after. Next was the VerduTex surface with 3µm diamond suspension; contained in a small plastic spray bottle and was sprayed on manually. To determine if enough has been added, the surface was wet when touched. Next surface used was the VerduTex surface with 1µm diamond suspension, and finally, the ChemoTex surface with 0.06µm diamond suspension. The abrasive used was scraped off the ChemoTex surface // or else the salt from the abrasive will crystallize on the surface. Once the polishing process was completed, the Buehler polisher equipment was turned off.

### 2.2.4 SEM images taken on polished sample

A scanning electron microscope (SEM) was used to analyze the polished, collected wafer. Several images were taken, and scaled appropriately in nanometers. The best images selected were kept, and determined the most contrast with other wafers.

## **2.3 Electrical Switch**

### 2.3.1 Research Objectives

To investigate Pulsed Reverse Current Protocol's application in silicon electrodeposition we will: Construct and implement a lab scale circuit model which periodically reverses polarity across an electrolytic cell with voltages ranging from 0.1-5V, currents ranging from 0.1-30A, a switching frequency of 1kHz, and a duty cycle of 96.67%.

### 2.3.2 Lab-Scale Model

#### **Purpose**

Constructing a lab scale model will allow us to observe the effects of PRPC on silicon electrodeposition as well as experiment with various input conditions. The findings from this experimentation will be considered to provide more insightful recommendations when investigating the model's industrial scalability. Before constructing the switching device, we will select components, describe the circuit construction process, and characterize the circuit's behavior under various testing conditions.

#### **Component Selection**

H-bridge circuits can be constructed with most common types of transistors, including BJTs (Bipolar Junction Transistors), MOSFETs (Metal Oxide Semiconductor Field Effect Transistors) and IGBTs (Insulated Gate Bipolar Transistors). The most suitable choice depends on the operating conditions, as each transistor possesses unique characteristics which influence their suitability for various applications. For high power applications, IGBTs and MOSFETs are

the component of choice as they can switch large currents with relatively low control voltages. Essentially, this means they offer low power control of high-power circuits, an especially attractive attribute, both in terms of efficiency and ease of use. While both components are suitable for the physical construction of the conceptual circuit, MOSFETs may be better suited for lab-scale experimentation as they are more economical and can accept a greater variety of input signals. However, IGBTs are better suited for industrial scale applications once specific input parameters have been identified.

MOSFETs are available in two different varieties, PMOS and NMOS devices, the P and N refer to the type of doped silicon each is composed of. With PMOS devices, charge is carried through electron holes, while NMOS rely on the more traditional transport of electrons. Because of these differences NMOS carry charge slightly faster and generally possess lesser resistance values when activated, which allows them to produce sharper signals with lower resistive losses. Minimizing resistive losses is not only important for system efficiency, but also for thermal performance. Resistance values in the switching components can dissipate substantial amounts of power in the form of heat. If unaccounted for, the resulting temperature rise can damage the MOSFETs as well as the circuit board. For these reasons, we used NMOS devices in our circuit construction.

MOSFET current throughput depends on the proportion of voltage applied across its gate terminal to the voltage applied across its drain and source terminals. Depending on the component's location within the circuit as well as operating conditions, it will require various voltages across its gate terminal, with some conditions requiring the gate voltage to be larger than that of the circuit's supply. Additionally, because our lab scale circuit exclusively uses NMOS devices, it will require an inverted control signal for one pair of MOSFETs. To accommodate this, the circuit will utilize an H-Bridge driver, which translates the control signal to the appropriate voltage and current levels to activate each MOSFET device. This allows for much greater versatility on the control side, as even very low power signals can activate the MOSFETs. These drivers are readily available as single package integrated circuits and will allow the circuit to adapt autonomously to various supply conditions.

## **Circuit Construction**

After suitable components were chosen, the circuit was constructed in Multisim, a digital circuit simulation software. Once the circuit's theoretical operation was verified, the digital schematic was exported to Ultiboard, a printed circuit board (PCB) design software, where a corresponding PCB layout was created. Several components used did not have an existing footprint in the software and had to be designed using their component specific datasheets. The completed layout was then sent to an online manufacturer, ALL PCB, who physically implemented the design and returned the physical PCB. Once received, the selected components were soldered onto the PCB by hand, using a soldering iron. This completed the construction of the board.

### **Behavior Testing and Circuit Characterization**

With a physical model constructed, our next step was verifying the circuit's behavior. To accomplish this, we first generated the device's simulated outputs using Multisim digital circuit simulation software. Using the simulated values as our expected output, we subjected the circuit to identical conditions and measured its real-world response. By comparing our simulated and expected values, we could determine whether the circuit was operating as desired. Specifically, we measured the deviations between the control signals and the output across the load. Additionally, we investigated the circuit's thermal performance when subject to large currents,  $5A < I < 22A$ .

For safety reasons, the initial testing was performed using low current  $\sim 0.1A$  and high voltage  $\sim 5V$ . Using an oscilloscope, we first measured the two control signals to ensure the microcontroller was outputting the appropriate waveforms. After the control signals were verified, a test circuit was constructed using a  $1k\Omega$  resistor as a test load and a benchtop power supply as a power source. An oscilloscope probe was connected across this load to measure its voltage. Additionally, we used control signals with various frequency and duty cycles to identify the device's operating range.

For thermal performance, we first constructed a test load capable of withstanding large currents. We started by mounting a  $100W$ ,  $0.2\Omega$  shunt resistor to an aluminum heat sink using thermal paste, to maximize contact area, and a zip tie, to further secure the resistor in place. After

constructing the test load, we created wires capable of handling the large currents. To achieve this, we connected two 12-gauge wires in parallel. Each 12-gauge wire is rated for a maximum of 20A, so a parallel combination of two provided the ability to carry 40A, leaving a comfortable margin for safety. With a test load and the appropriate wiring in place, we connected the test load and the power supply to the switch's corresponding terminals. We then proceeded to slowly increase the current supply until we reached the load's maximum of ~22A.

## Chapter 3: Results and Discussion

### 3.1 Life Cycle Analysis

#### 3.1.1 Siemens Process vs Electrolysis

When comparing the environmental impacts of the Siemens process to the molten Salt Electrolysis using their respective life cycle analysis, the first step was to ensure that the scope of the information for each process was the same. The life cycle analysis for the Siemens process that the Molten Salt electrolysis process is being compared to is what is called a gate to gate process, meaning the environmental impacts being observed are only those directly involved in the process itself rather than a cradle to gate which takes into account the source of each of the materials as well. Because the process created for the Molten Salt Electrolysis is a cradle to gate life cycle analysis, this needed to be amended for the comparison to be valid. For the purpose of the comparison, both the environmental impacts of the Siemens process and the Molten Salt Electrolysis will be from their gate to gate processes. All of the impacts will be based on the production per kg of solar grade silicon.

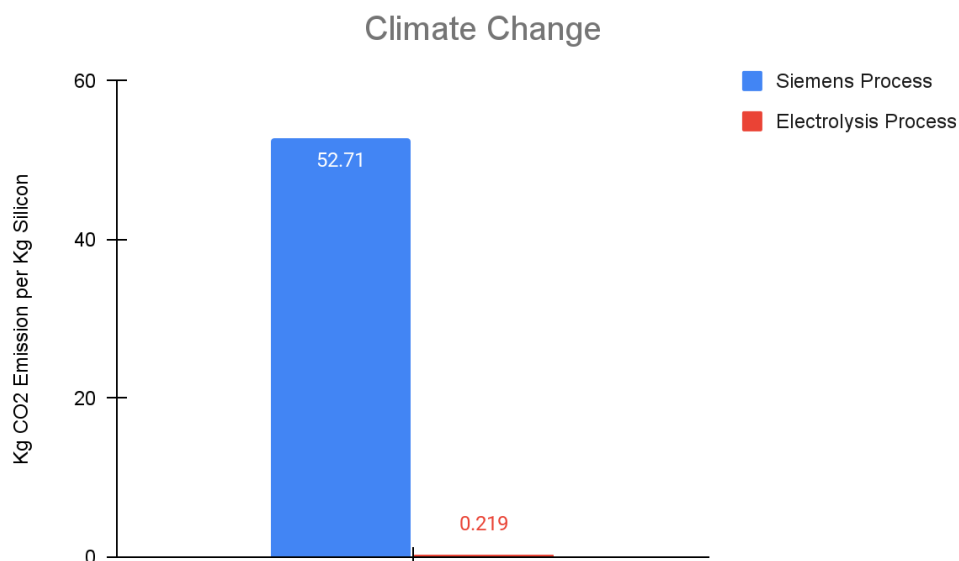


*Figure 22: Comparison of climate change impact between the Siemens process and the Molten Salt Electrolysis process.*

The first impact factor to analyze is the climate change category. This factor directly measures how much carbon dioxide is released into the atmosphere as a direct result of the process. As seen in figure 22, the amount of CO<sub>2</sub> released into the atmosphere as a result of the Siemens process per kg of solar grade silicon produced is 52.71 kg. This same factor analyzed for the Molten Salt Electrolysis results in a total amount of CO<sub>2</sub> released of 0.219 kg per kg of solar grade silicon produced. There are a number of factors that contribute to this large difference in environmental impact. The first of these is that the molten salt electrolysis process is designed to be more efficient than the Siemens process which has not historically been a very efficient process at all but is currently just the best option available. The Molten Salt Electrolysis process is designed to incorporate hydroelectric power and does not include many of the electricity intensive steps that are necessary for the Siemens process. The main drawback to the Molten Salt Electrolysis in this category is that its scalability is still largely unknown which means that this estimation may be very optimistic. This analysis also does not take into account the transportation of the many materials required to make up the salt bath, all of which will also contribute to the environmental impact.

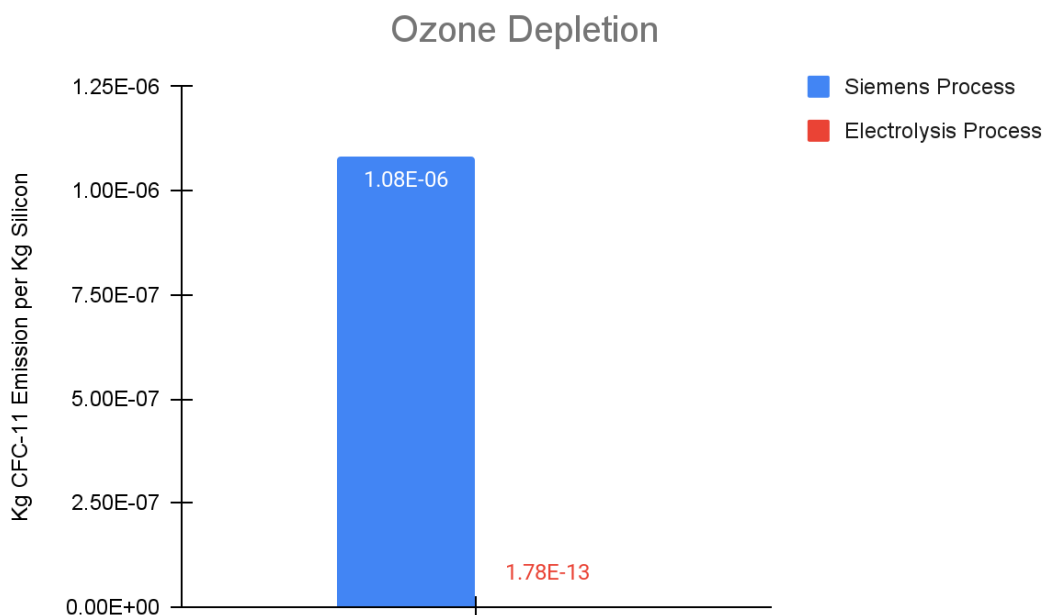


*Figure 23: Comparison of effects on Ozone Depletion between the Siemens process and the Molten Salt Electrolysis process.*



Another impact factor to analyze is the amount of ozone depletion. This relates to the amount of CFC, chlorofluorocarbons, being released into the atmosphere. As shown in figure 23, while neither process produces a significant amount of CFCs, the Molten Salt electrolysis again has significantly less of an impact when compared to the Siemens process. This is again due to many of the reasons mentioned above, however based on the processes involved in the molten salt electrolysis, it is not reasonable for a buildup of CFCs to be a major concern for the process.

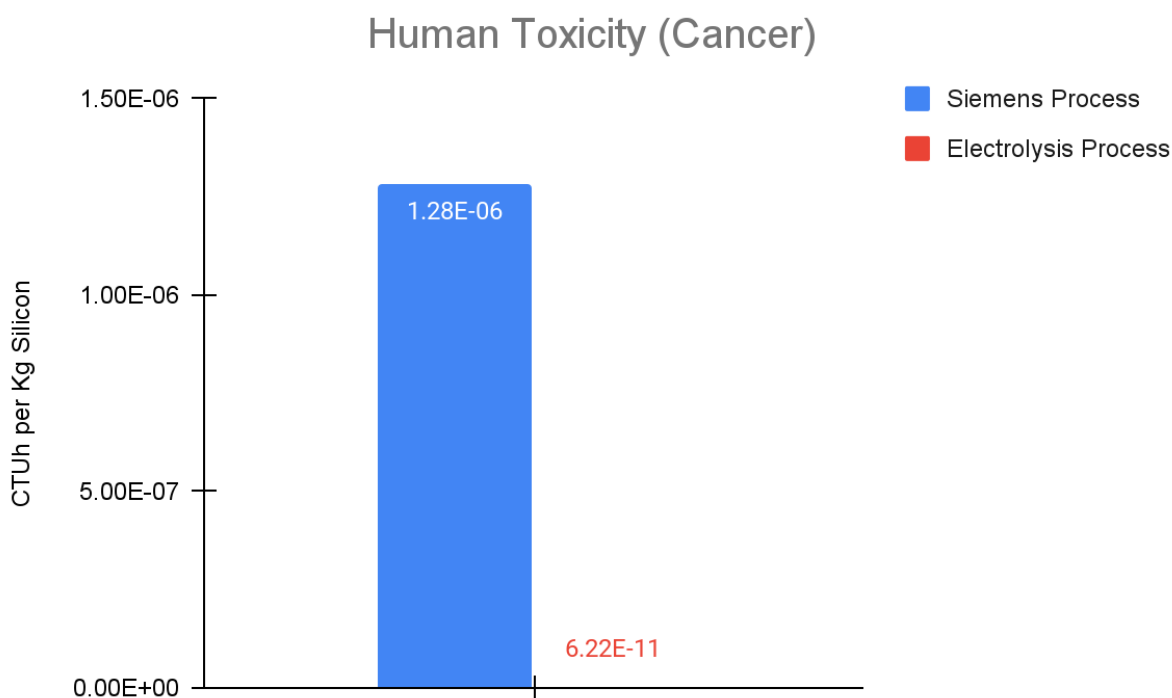


*Figure 24: Comparison of human toxicity, cancer, between the Siemens process and the Molten Salt Electrolysis process.*

One final impact factor that was analyzed was the toxicity to humans of the process. This was done by measuring the amount of 1,4 dichlorobenzene released per 1 kg of solar grade silicon. As with the other two factors analyzed, the molten salt electrolysis was superior in its lack of emissions to the Siemens process. Based on these factors that were analyzed, if the molten salt electrolysis method can be scaled up in a way that is economically feasible, it will have a clear environmental benefit over the Siemens process.

### 3.1.2 Comparison of electrolysis components environmental effects

The compiled results from the LCA are shown below in Table 2 using the Environmental Footprint Mid-Point assessment methods. The scope of the assessment is cradle-to-gate encompassing raw material extraction, mineral processing, transportation, fuel production, and final solar silicon production. The impacts from the various categories were allocated into groupings that represent the productions' subprocesses. For the material inputs (CaF<sub>2</sub>, MgF<sub>2</sub>, CaO, SiO<sub>2</sub>, and Y<sub>2</sub>O<sub>3</sub>) this includes raw material extraction, intermediate production steps, and transportation up to the final solar silicon facility. The "Solar Silicon Electrolysis Process" group accounts for the impacts at the facility and the energy use that the plant requires. "Fuel production" incorporates the full supply chain for the manufacturing of the various liquid fuels such as diesel used by trucks and trains, and heavy fuel oil for container ships. In general, "MgF<sub>2</sub>" has the largest environmental impact for every kg of solar silicon product. Out of 19 impact categories, magnesium fluoride production was the highest for 16 of those indicators. The largest contributor for the remaining categories are split amongst the "Solar Silicon Electrolysis Process", "SiO<sub>2</sub>", and "Fuel Production". The smallest contributor was "Y<sub>2</sub>O<sub>3</sub>" followed by "CaO". A more detailed assessment follows that highlights three impact categories that include climate change, human toxicity cancer, and ozone depletion.

*Table 2: Midpoint indicator results from the cradle-to-gate life cycle assessment of the input streams for the solar silicon production via electrolysis per kg of solar silicon product (Environmental Footprint Mid-Point indicator).*

		Process	Solar Silicon Electrolysis Process	CaF2	MgF2	CaO	SiO2	Y2O3	Fuel Production
<b>Flow</b>	<b>Category</b>								
Acidification	mol H+ eq		7.24E-05	0.000486	0.00262	2.10E-06	0.000188	6.88E-06	9.14E-05
Climate change	kg CO2eq		0.219	0.0557	0.249	0.00478	0.0893	0.000863	0.0148
Climate change-Biogenic	kg CO2eq		2.38E-05	1.59E-06	0.000180	1.77E-06	4.33E-05	3.55E-08	0.000151
Climate change-Fossil	kg CO2eq		0.219	0.0557	0.249	0.00478	0.0892	0.000863	0.0141
Climate change-Land use and land use change	kg CO2eq		3.16E-05	6.37E-06	5.31E-05	8.33E-07	1.40E-05	3.14E-07	0.000614
Ecotoxicity, freshwater	CTUe		0.00194	0.0331	1.94	2.47E-05	0.00234	0.000535	0.0153
Eutrophication marine	kg N eq		2.03E-05	7.94E-05	0.000340	9.11E-07	7.42E-05	8.27E-07	2.29E-05
Eutrophication, freshwater	kg P eq		4.83E-08	6.36E-09	4.97E-05	1.34E-09	3.62E-08	1.92E-10	5.38E-07
Eutrophication, terrestrial	mol N eq		0.000221	0.000871	0.00374	9.81E-06	0.000812	9.13E-06	0.000214
Human toxicity, cancer	CTUh		6.22E-11	6.63E-10	1.94E-08	3.46E-12	8.19E-11	6.20E-12	6.00E-10
Human toxicity, non-cancer	CTUh		2.30E-09	2.15E-09	1.15E-07	3.48E-10	8.39E-10	9.84E-11	8.07E-09
Ionising radiation, human health	kB1 U235 eq		0.000515	0.000243	0.00937	2.97E-05	0.00430	4.11E-06	0.000368
Land use	m2a		0.0172	0.0684	1.07	0.00347	0.921	0.00989	0.149
Ozone depletion	kg CFC-11 eq		1.78E-13	1.49E-13	2.21E-10	7.46E-16	3.74E-12	1.54E-16	3.26E-13
Particulate Matter	PM2.5 eq		1.40E-09	2.90E-07	2.93E-08	1.60E-11	4.27E-06	4.60E-10	7.24E-10
Photochemical ozone formation - human health	kg NMVOC eq		5.69E-05	0.000193	0.00100	2.08E-06	0.000224	2.56E-06	5.62E-05
Resource use, fossils	MJ		0.171	0.362	2.59	0.0138	1.38	0.00869	1.18
Resource use, minerals and metals	kg		1.67E-06	1.62E-09	6.49E-06	1.43E-10	6.25E-09	3.61E-11	1.01E-08
Water use	m3		1.68	0.00476	0.114	3.90E-06	0.00209	0.00168	0.00331

\* - Green fill indicates the largest contributor and orange signifies the smallest within each impact category.

Climate change is the first impact factor to be analyzed from the impact assessment categories. The units for climate change are expressed in kg of CO<sub>2</sub>eq (CO<sub>2</sub> equivalence). This uses the Bern model and considers other greenhouse gasses and converts them to their CO<sub>2</sub> equivalence based on their global warming potential over a 100 year time horizon (Manfredi et al., 2012). As shown in Figure 25, the full process stream for MgF<sub>2</sub> is responsible for 39% of the impact on climate change. For 1 kg of solar silicon product, the MgF<sub>2</sub> stream produces 0.249 kg of CO<sub>2</sub>eq with the Solar Silicon Process second producing 0.219 kg of CO<sub>2</sub>eq. Magnesium fluoride is used in the highest quantity relative to the other salt bath components, explaining why it is such a large contributor. The magnesium fluoride process stream is also very complex and features a variety of sub-processing steps to go from MgO and HF to make MgF<sub>2</sub>. This inherently requires lots of transportation to move the materials between facilities. The majority of this transportation is conducted via diesel trucks. The process to convert MgO and HF into MgF<sub>2</sub> was not included in the various open-source databases therefore it is likely that the actual climate change impact for this stream is higher. Using the contribution tab within OpenLCA, it is evident that the majority of the emissions from the preparation of magnesium fluoride are attributed to the production of HF and MgO. The process of making magnesium oxide involves the calcination of magnesium carbonate using a large kiln. There are both direct and indirect emissions from calcination. Direct emissions are from the conversion of magnesium carbonate to magnesium oxide producing carbon dioxide as a byproduct. The indirect emissions are related to the emissions from the fuel that is used for the kiln. Hydrogen fluoride production starts with mining of calcium fluoride and is combined with sulphuric acid in an endothermic reaction. The process is very energy intensive and begins with the reaction taking place in a kiln. Facilities will condense and then distill the product to make high purity HF requiring large amounts of energy to operate. The energy used is a mixture of fuels and electricity leading to indirect CO<sub>2</sub> emissions from their usage. The solar silicon electrolysis process was the second largest contributor which is mainly due to its high electricity usage. The electricity for the process is supplied by hydroelectric power which produces negligible emissions in itself. However, the process from the Environmental Footprint database includes the construction of the dam and facility in its

assessment. Since dams are mostly comprised of concrete, there is a large amount of CO<sub>2</sub> produced as a result. The processes with the lowest impact on climate change were yttrium oxide producing  $8.63 \times 10^{-4}$  kg of CO<sub>2</sub>eq and calcium oxide  $4.78 \times 10^{-3}$  kg of CO<sub>2</sub>eq per kg of final solar silicon product. Both chemicals are used in relatively smaller amounts explaining their insignificant impact on climate change.

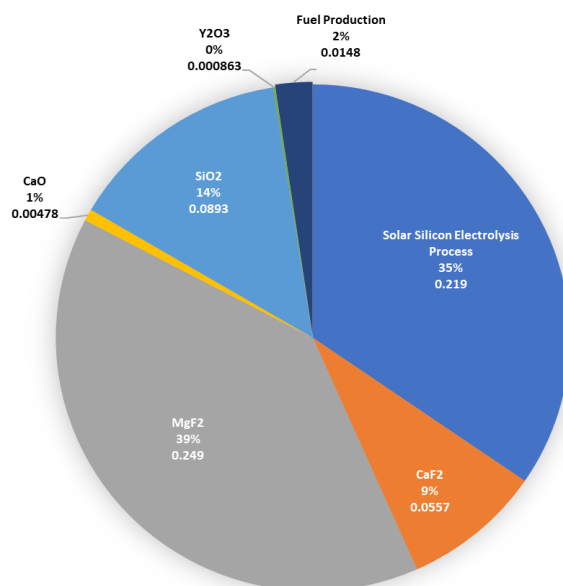
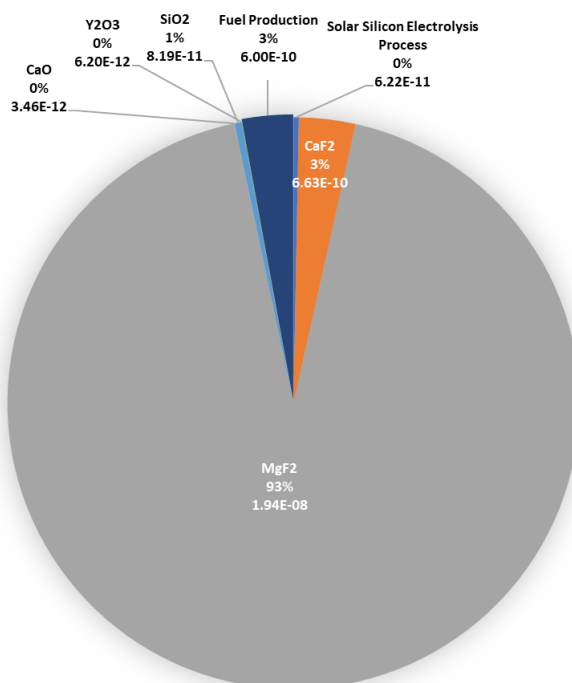


Figure 25: Percentage contribution of the process streams towards climate change in units of kg of CO<sub>2</sub>eq (CO<sub>2</sub> equivalence).

Human toxicity cancer is the second impact factor to be assessed from the impact assessment categories. The units for human toxicity cancer are provided in CTUh (Comparative Toxic Unit for humans) as indicated in Table 2 (Manfredi et al., 2012). The comparative toxic unit for humans is calculated using the USEtox model which estimates the increase in death in the total human population per 1 kg of manufactured solar silicon (“What are the units”, 2022). Magnesium fluoride production is overwhelmingly the dominant contributor to human toxicity cancer as shown in Figure 26. For every kilogram of solar silicon produced, magnesium fluoride production increases mortality by  $1.94 \times 10^{-8}$  persons. Considering a full-scale silicon plant which would theoretically produce 160,000 metric tons of solar silicon a year, that would equate to an increase in mortality of 3.104 people due to magnesium fluoride production. The actual impact is

likely to be higher since the process to convert  $\text{MgO}$  and  $\text{HF}$  into  $\text{MgF}_2$  was not included in this version of the life cycle assessment. Considering the processes available, hydrogen fluoride production is a small contributor at about 16% while magnesium oxide production is responsible for approximately 75% of the impact on human health. Magnesium oxide's human health impact is the result of waste products that collect in the water that is used in the washing of the raw material. Chemicals found in the wastewater include chromium-6, arsenic-5, and nickel which are all toxic and detrimental to human health. The processes with the lowest impact to human health were yttrium oxide and calcium oxide which increased mortality by a negligible amount compared to other streams. As mentioned previously, both compounds are used in relatively smaller amounts explaining their insignificant impact on human health.



*Figure 26: Percentage contribution of the process streams towards human toxicity, cancer in units of CTUh (Comparative Toxic Unit for humans).*

The last impact factor to be analyzed from the impact assessment categories is ozone depletion. The units for ozone depletion are provided in kg of CFC-11eq (Trichlorofluoromethane) as shown in Table 2. The Environmental Footprint assessment method uses the EDIP model which is based on the ozone depletion potentials(ODP) provided by the

World Meteorological Organization(WMO) over an infinite time horizon (Manfredi et al., 2012). The WMO has identified 21 man-made chemicals referred to as Ozone Depleting Substances(ODS) that include fluorine, bromine, and chlorine groups. The ODP relates the amount of ozone destroyed by a particular chemical during its lifetime to the amount of ozone destroyed by CFC-11(Trichlorofluoromethane) during its lifetime (Steinmann & Huijbregts, n.d.). The EDIP model uses the ODPs to output the trichlorofluoromethane equivalence in kilograms of the various ozone-depleting chemicals. Based on the model, magnesium fluoride production is responsible for 98% of the impact on ozone depletion as shown in Figure 27. Hydrogen fluoride production contributes 96% while magnesium oxide contributes a smaller percentage of 2%. The impact from the hydrogen fluoride production can be traced to the emissions of chlorofluorocarbons, hydrochlorofluorocarbons, and 1,1,2-trichlorotrifluoroethane. These chemicals are emitted to the air likely as a byproduct during the distillation process of hydrogen fluoride production. Magnesium oxide production also produces chlorofluorocarbons and hydrochlorofluorocarbons but at a much smaller quantity. In comparison, the processes with the lowest impact on ozone depletion were yttrium oxide, calcium oxide, and solar silicon electrolysis process. The solar silicon process only emits to the air oxygen gas explaining its low impact on ozone depletion. The process of preparing yttrium oxide is chemically intensive and emits a series of ozone depleting chemicals into the air. However, its impact, like calcium oxide, is minimal due to the small quantity that is required for the molten salt bath.

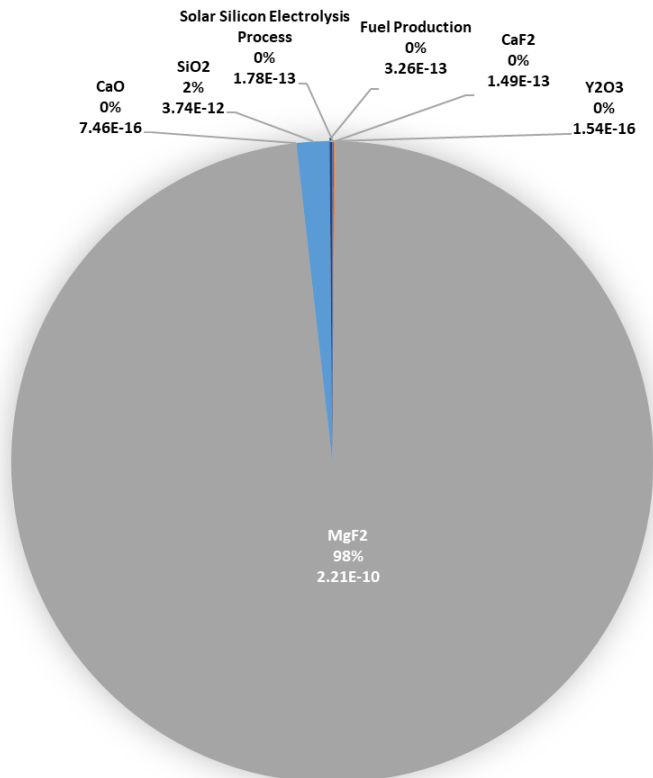


Figure 27: Percentage contribution of the process streams towards ozone depletion in units of kg of CFC-11eq (Trichlorofluoromethane equivalence).

### 3.1.3 Contribution Analysis

Table 3: Environmental Footprint (Mid-point indicator) results for transportation, mining and refinement, and solar silicon production for molten electrolysis process.

		Transportation	Mining and Refinement	Solar Silicon Production
Flow	Category			

Acidification	mol SO2 eq	3.36E-04	3.05E-03	7.24E-05
Climate Change	kg CO2 eq	0.08588388302	0.3278734754	0.2189056644
Climate Change- Biogenic	kg CO2 eq	1.51E-04	2.26E-04	2.38E-05
Climate Change- Fossil	kg CO2 eq	0.08511885562	0.3275727214	0.2188502839
Climate Change- Land use and land use change	kg CO2 eq	6.14E-04	7.43E-05	3.16E-05
Ecotoxicity, freshwater	Item(s) 1.4 DB eq	0.01531935314	1.977022586	0.001939954669
Eutrophication, marine	kg N eq	1.50E-04	3.67E-04	2.03E-05
Eutrophication, freshwater	kg P eq	5.38E-07	4.98E-05	4.83E-08
Eutrophication, terrestrial	mol N eq	1.62E-03	4.04E-03	2.21E-04
Human toxicity, cancer	Item(s) 1,4 -DB eq	6.00E-10	2.01E-08	6.22E-11
Human toxicity, non-cancer	Item(s)	8.07E-09	1.19E-07	2.30E-09
Ionizing radiation, human health	kBq U235 eq	3.68E-04	0.01394415676	5.15E-04
Land use	Item(s) m2a	0.1494032012	1.557262496	0.01436615174



Ozone depletion	kg CFC-11 eq	3.26E-13	2.25E-10	1.78E-13
Particulate Matter	Item(s) PM10 eq	5.66E-09	4.59E-06	1.40E-09
Photochemical ozone formation- human health	kg ethylene eq	2.83E-04	1.19E-03	5.69E-05
Resource use, fossils	MJ	1.18	4.345129908	0.1705297687
Resource use, minerals and metals	kg	1.01E-08	6.50E-06	1.67E-06
Water use	m3	3.31E-03	0.1208685967	1.681392095

*Table 4: Percent contribution for each contributor towards the environmental footprint (mid-point indicator).*

	Percent Contribution by Category		
	Transportation	Mining and Refinement	Silicon Production
Acidification	9.71	88.19	2.09
Climate Change	13.57498067	51.82434623	34.6006731
Climate Change- Biogenic	37.69	56.37	5.93

Climate Change- Fossil	13.47794357	51.86872663	34.65332981
Climate Change- Land use and land use change	85.28	10.33	4.39
Ecotoxicity, freshwater	0.7681638783	99.13456027	0.09727585026
Eutrophication, marine	27.93	68.30	3.77
Eutrophication, freshwater	1.07	98.84	0.10
Eutrophication, terrestrial	27.49	68.74	3.76
Human toxicity, cancer	2.89	96.81	0.30
Human toxicity, non-cancer	6.25	91.98	1.78
Ionizing radiation, human health	2.48	94.05	3.47
Land use	8.681024773	90.48423462	0.8347406088
Ozone depletion	0.14	99.78	0.08
Particulate Matter	0.12	99.85	0.03
Photochemical ozone formation-human health	18.52	77.75	3.72
Resource use, fossils	20.68	76.32444063	2.995443055
Resource use, minerals and metals	0.12	79.50	20.38

Water use	0.18	6.69	93.12
-----------	------	------	-------

In the contribution analysis we can group the scope of the life cycle of silicon production into three main categories:

1. Raw material extraction and refinement
2. Transportation
3. Silicon Production

In this section of the analysis, the tables and details can be found in the supplementary material seen in Table 3, and 4.

From the results given in OpenLCA, raw material extraction and refinement contributes the highest percentage towards any of the environmental footprint indicators being analyzed with more than 50% contribution from 17 out of the 19 categories except for water use as well as climate change caused by land use and land use change. Due to the environmentally unfriendly sub processes included in mining and refinement, more specifically for magnesium fluoride production and rare earth mining in general, these results would be expected. Based on the total amount of silicon planned to be produced by the plant, this environmental footprint would likely increase, especially in regards to particulate matter in the locations in which these mines reside. Another factor to take into account for the mining and refinement process is the machinery being used to refine and move these materials. For example, drilling equipment, sifting machines as well as dump trucks contribute more in environmental impact due to the lubricating oil, and/or diesel being used to operate them as well as the process of shaking/shifting material, contributing more towards particulate matter being spewn into the air. Another factor to consider within these results is that of human toxicity. From these results, mining and refinement makes up 96.81% contribution towards human toxicity cancer and 91.98% human toxicity demonstrating that these mining practices not only harm the environment but the inhabitants that may be living close to the mine as well.

From the results it can be seen that transportation contributes the most in climate change land use and land use change. This makes sense due to the construction of roads, ports, and rails in order for materials to be transported. Surprisingly, it was found that transportation had the lowest overall impact for fossil fuel based climate change. The reasoning for this is that the amount of fuel used for the transportation of these materials is being better utilized by appropriately setting the utilization ratio within OpenLCA at 60%. This means that a majority of cargo space is being used in transport, reducing overall consumption of fuel. In addition to this, when comparing fuel use to that of silicon production, it can be seen that silicon production has a higher percent contribution towards fossil based climate change than that of transportation. This is most likely due to the fossil fuels being used in the construction of a dam meant to provide hydroelectric power to the silicon plant. Transportation also accounted for larger percent contributions in expected categories such as photochemical ozone formation at 18.52% and resource use fossils at 20.68%. These contributions are still less than that of mining and refinement but over time we expect those contributions to increase as materials are consistently being brought to the plant for production. In order to reduce the environmental impacts of transportation, mines closer in vicinity could be utilized, shortening traveling distances and reducing overall impact in every category. Within this life cycle analysis this was considered, but locations of the mines could change in the future based on what is most cost effective and/or closest.

Silicon production contributed the least in 14 out of the 19 environmental impact categories except for water use, climate change, climate change fossil, ionizing radiation, and resource use minerals and metals within the contribution analysis. As previously mentioned, the climate change, and climate change fossil higher than expected percent contributions are most likely due to the construction of the dam meant to be used for hydroelectric power. Since this process also requires a wide array of salts for the salt bath, it would also make sense that silicon production would have the second highest percent contribution in the impact category of resource use of minerals and metals. Silicon production also had the highest percent contribution of water use out of the three main contributors. Due to the fact that the electricity source is from hydroelectric power, the water usage would be more than that of the mining and refinement category. The impacts from solar silicon production come mainly from the salt bath components

present in the process since they have to be transported to the plant but since the total amount of salt bath components are scaled for production of one kilogram of silicon, they contribute very little to the overall impact of the process. This would make sense as the process for solar silicon production using molten electrolysis only requires the inputs of the salt bath components and electricity through hydroelectric power. The design of this process is meant to be cheaper and performed in fewer steps than that of the Siemens process, so it's understandable that this would contribute less in most categories. A gate to gate comparison of these two silicon production methods will be discussed later outlining the specific differences between these two production methods.

### **3.2 Experimental Component**

On average, cracks and deformities on the pure silicon wafer were much higher than that of the coated silicon wafer, as shown in figure 22 and figure 23. Cracks in the uncoated silicon wafer extended around 70 nm whereas the coated wafer possessed cracks up to 40 nm. Further experiments will need to be run to confirm this correlation, but it can be deduced that the silicon nitride coated effectively resisted oxygenated corrosion on the silicon wafer during electrolysis.

Many experimental limitations are to be taken into account. The polishing on the coated silicon wafer was not effective and resulted in many scratches, which may deter any logical conclusions made. Additionally, crucible failure in the batch reactor caused delays up to several months, preventing more experiments to be run over the course of the project.



*Figure 28: Silicon wafer without coating.*

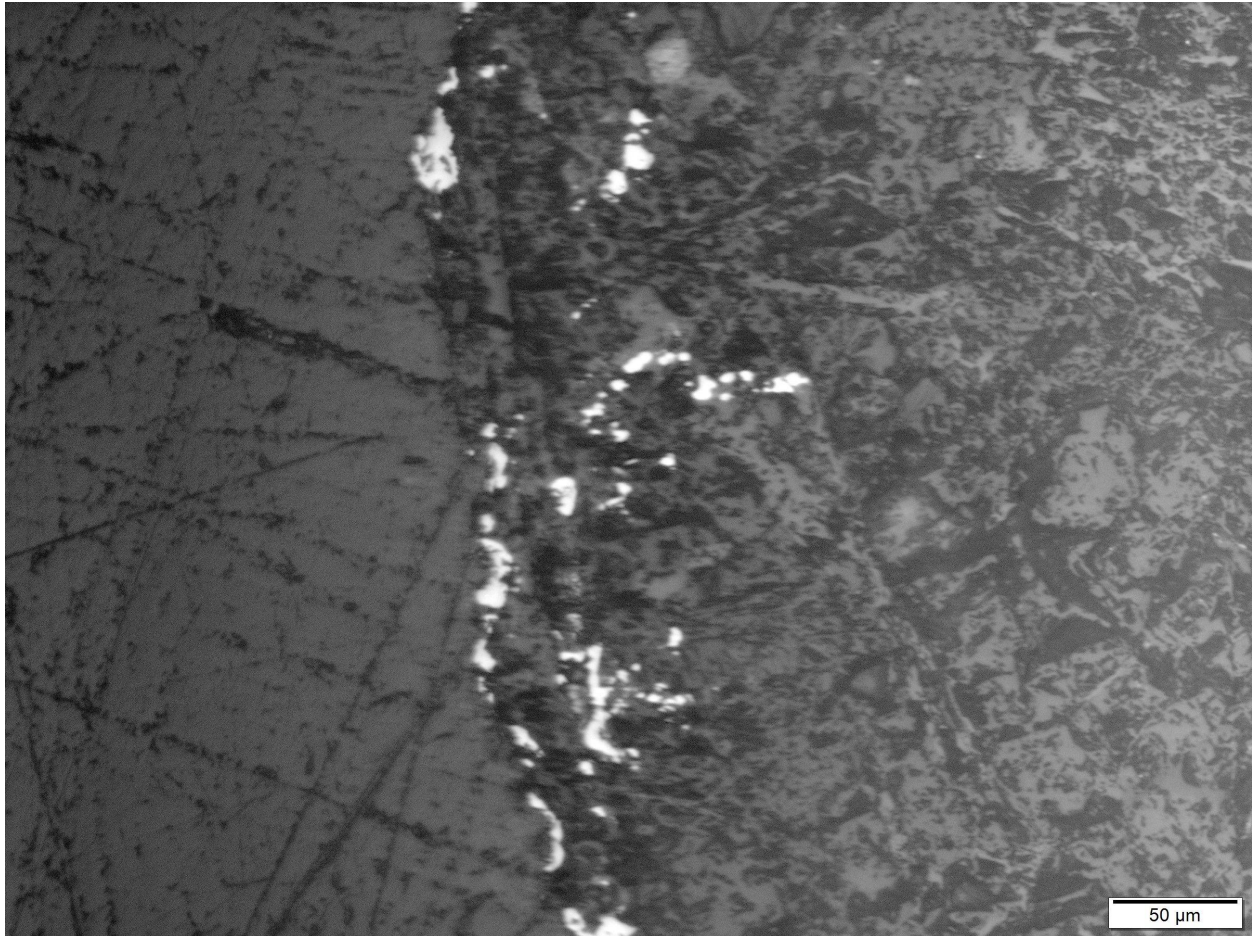


*Figure 29: silicon wafer with coating.*

Additionally, losing the wafer in the melt was an ongoing problem resulting from the cracks from oxygenated corrosion, physical flow and weight of the silicon yield; with more emphasis on the latter with the coated wafer. Sandpaper was used to grind off the silicon nitride coating in the dipped section (about 4 cm in), which allowed the pure silicon extract to be continuous.

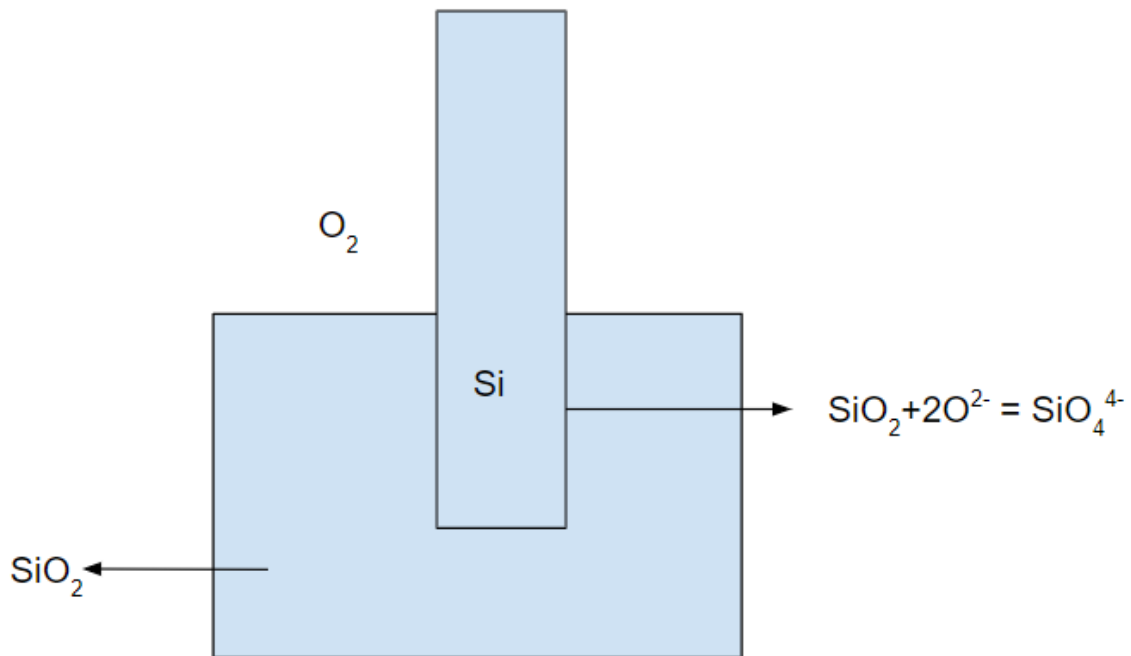


Figure 30: Oxygenated corrosion mechanism

Lastly, any corrosion falling back into the melt will not add any impurities, but instead add to the existing feed of  $SiO_2$ . Therefore, the only setback will be the wafer breaking, reducing potential yield immensely.

### **3.3 Electrical Switch**

#### Component Selection

The following components were selected for the design:

- MOSFETs
  - NTMFS0D5N03C
    - Single N-Channel Power MOSFET
    - $R_{ds} = 0.52 \text{ m}\Omega$
    - $I_{Max} = 464 \text{ A}$
    - $R\theta_{JA} = 38^\circ\text{C/W}$



At the proposed current levels, thermal rise can be calculated as:

$$\Delta T = R\theta JA * PDissipated$$

@30A, this would produce a ~20°C, or ~68°F rise in temperature.

The NTMFS0D5N03C was primarily selected for its low resistance value. This resistance value allowed the lab-scale model to forego a heat sink, greatly simplifying the construction and implementation process.

- IXFN200N10P
  - Single N-Channel Power MOSFET
  - Rds = 5.5 mΩ
  - IMax = 400A
  - RθJA = 0.27°C/W

While possessing a larger on resistance than the NTMFS0D5N03C, the XFN200N10P possesses a much lower thermal resistance. This substantially lesser thermal resistance combined with a heat sink, ensured the second iteration would run much cooler than the first, With a predicted rise of ~1°C.

- • H-Bridge Driver ICs
  - IR2104
    - Half-Bridge Driver
    - VMax = 600V
    - 10V < Vcc < 20V
    - Vin = 3.3V, 5V, 15V

The IR2104 was selected for its broad range of input voltages, which allow for flexibility on the circuit's control side, and its output voltage which is between 10V and 20V. While 5V logic level signals can activate a MOSFET, larger voltages further reduce the MOSFET's resistance, which assists with both efficiency and thermal stability.

### Circuit Construction

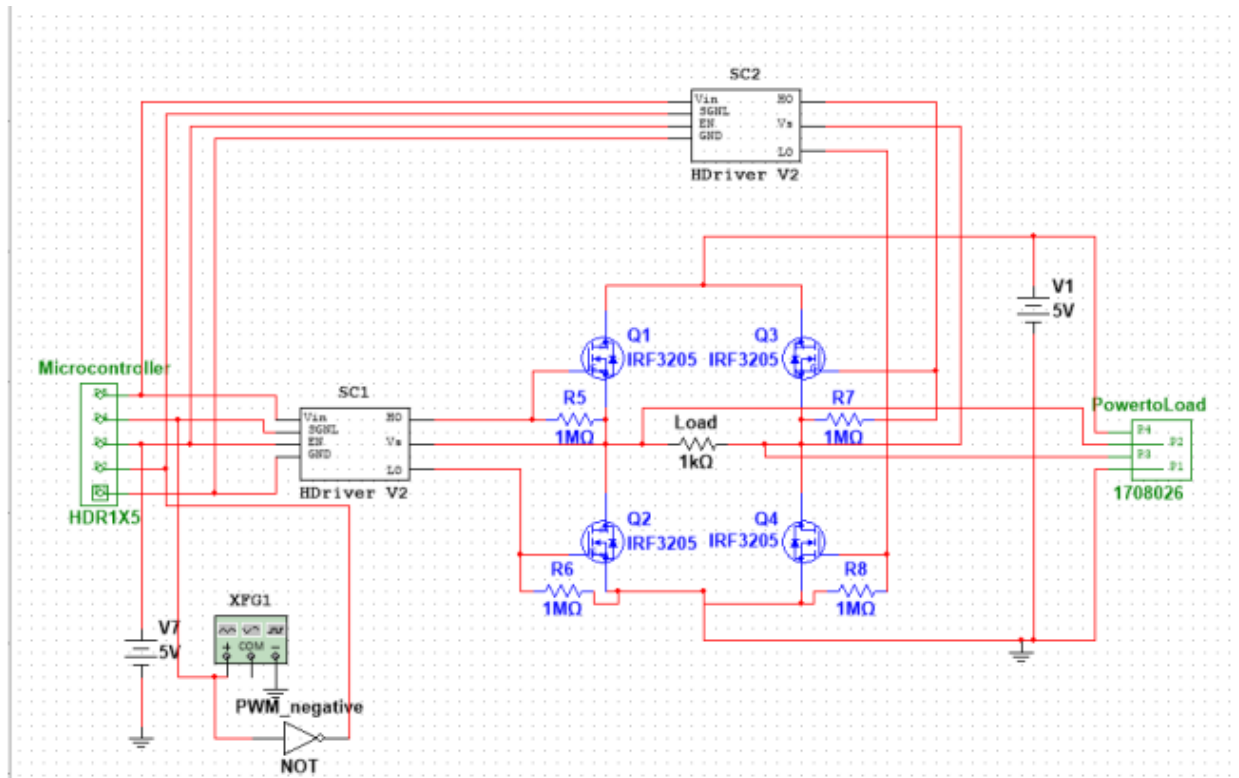


Figure 31: Simulated circuit model.

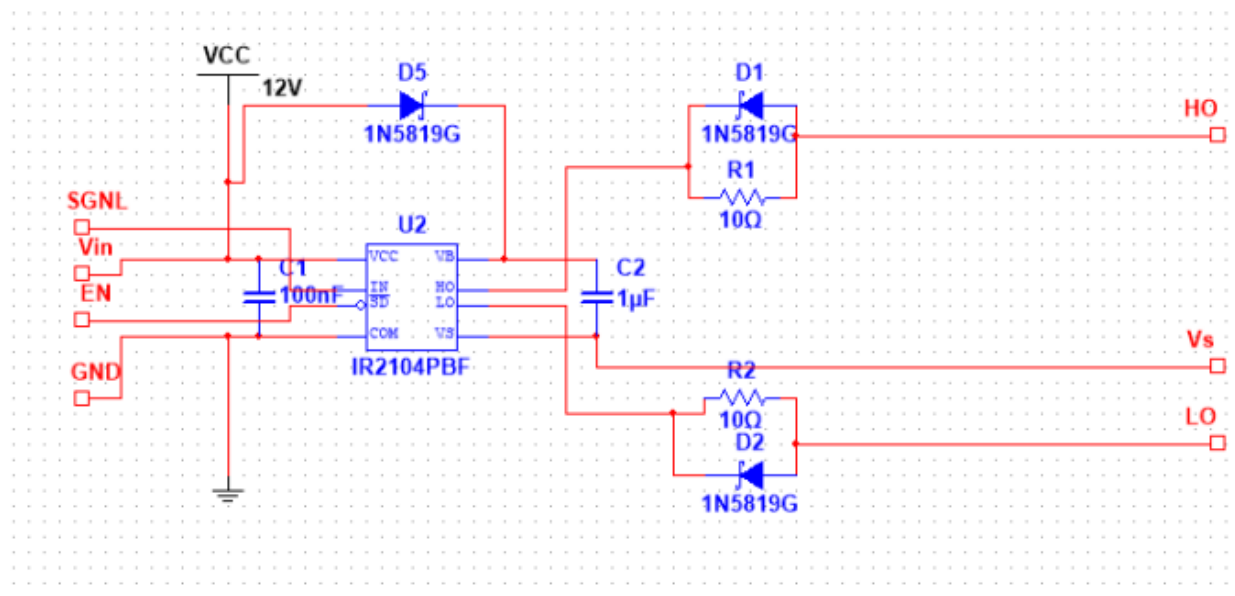


Figure 32: HDriver sub circuit of Figure 24.

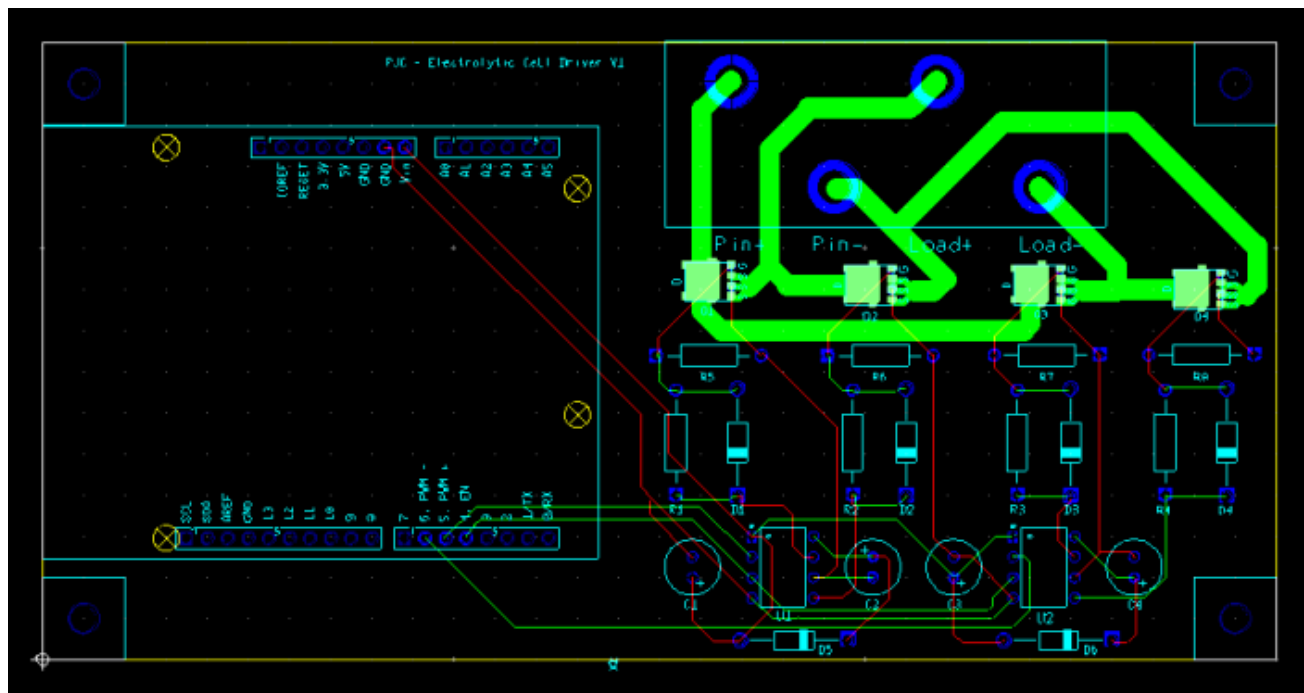


Figure 33: PCB Schematic for circuit in Figure 24.

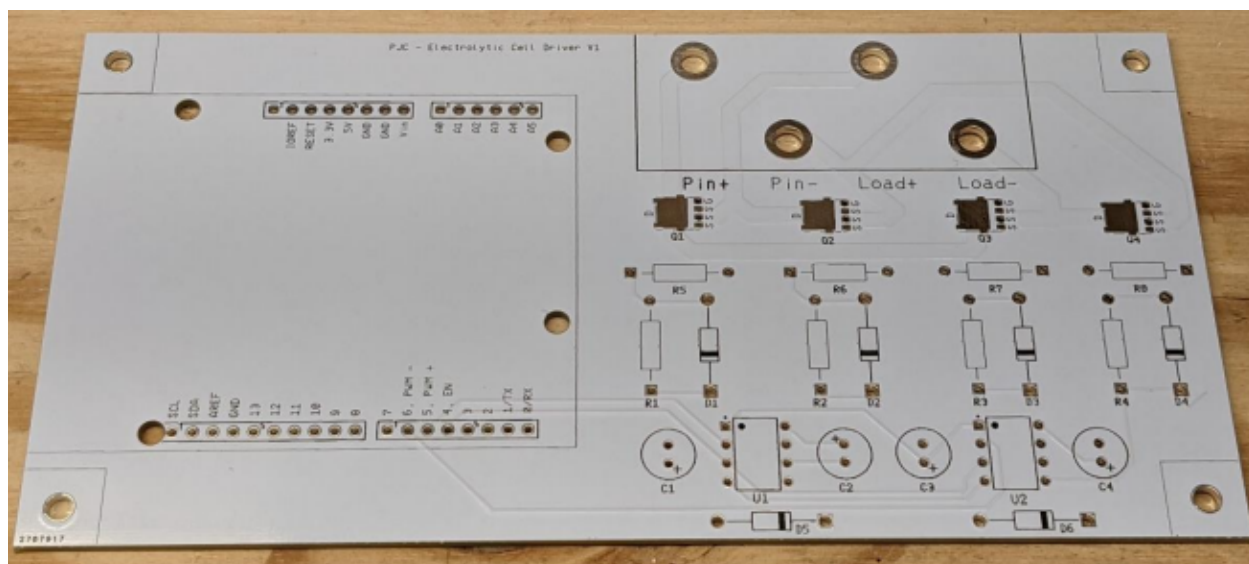


Figure 34: Blank PCB.

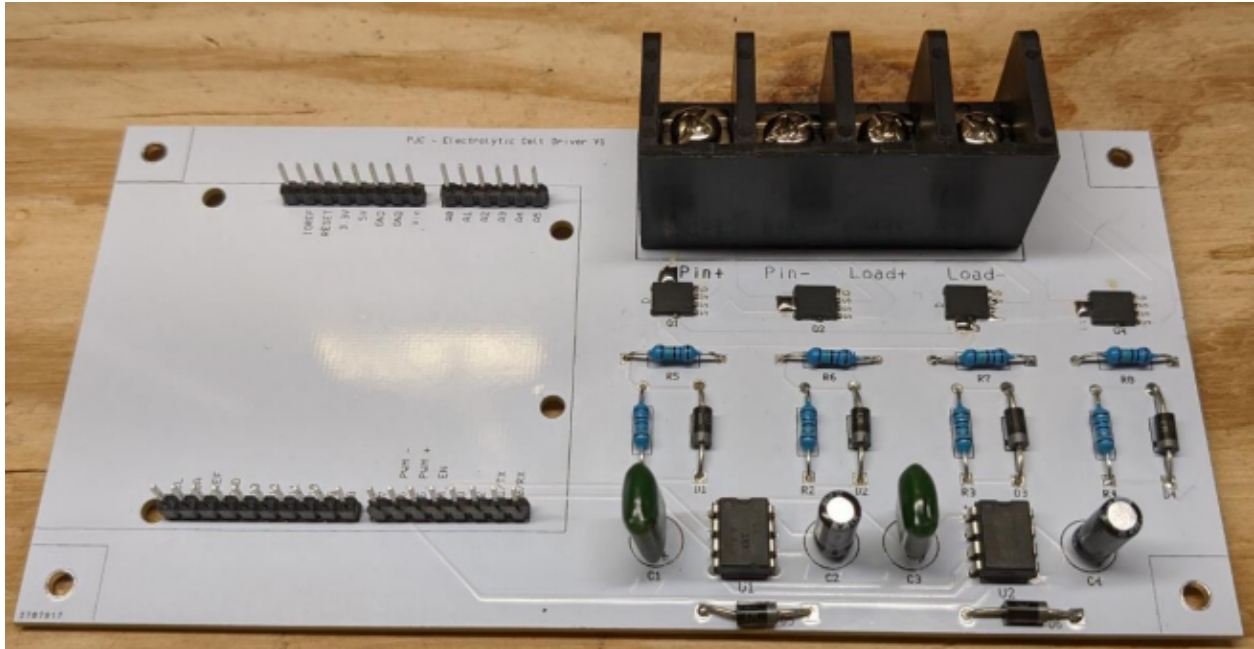


Figure 35: Constructed PCB.

### Behavior Testing and Characterization

#### Signal Testing-

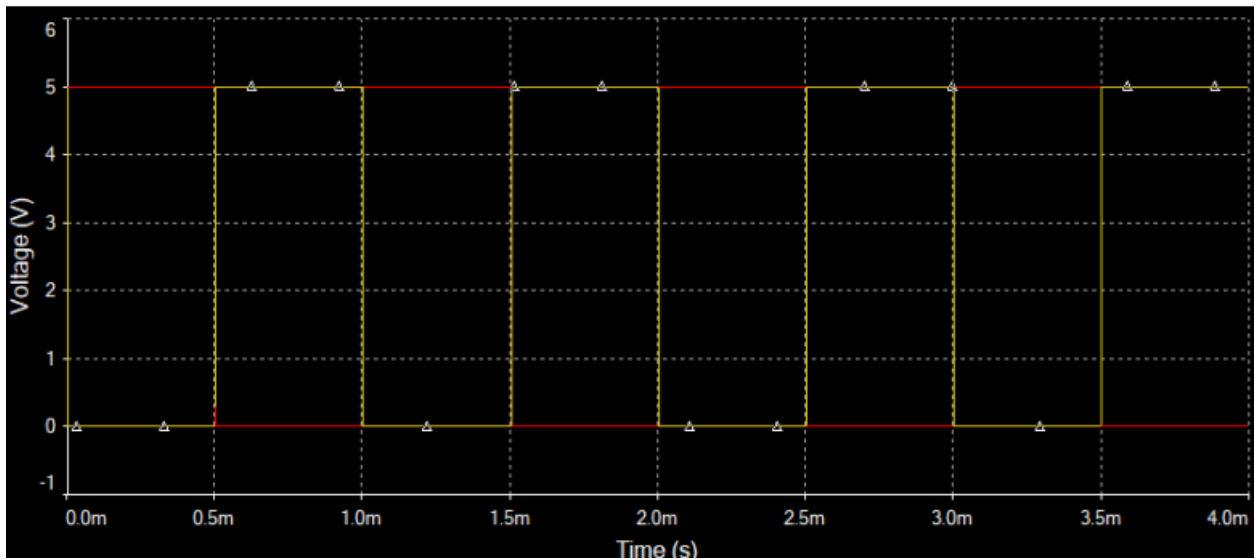


Figure 36: Simulated control waveforms.

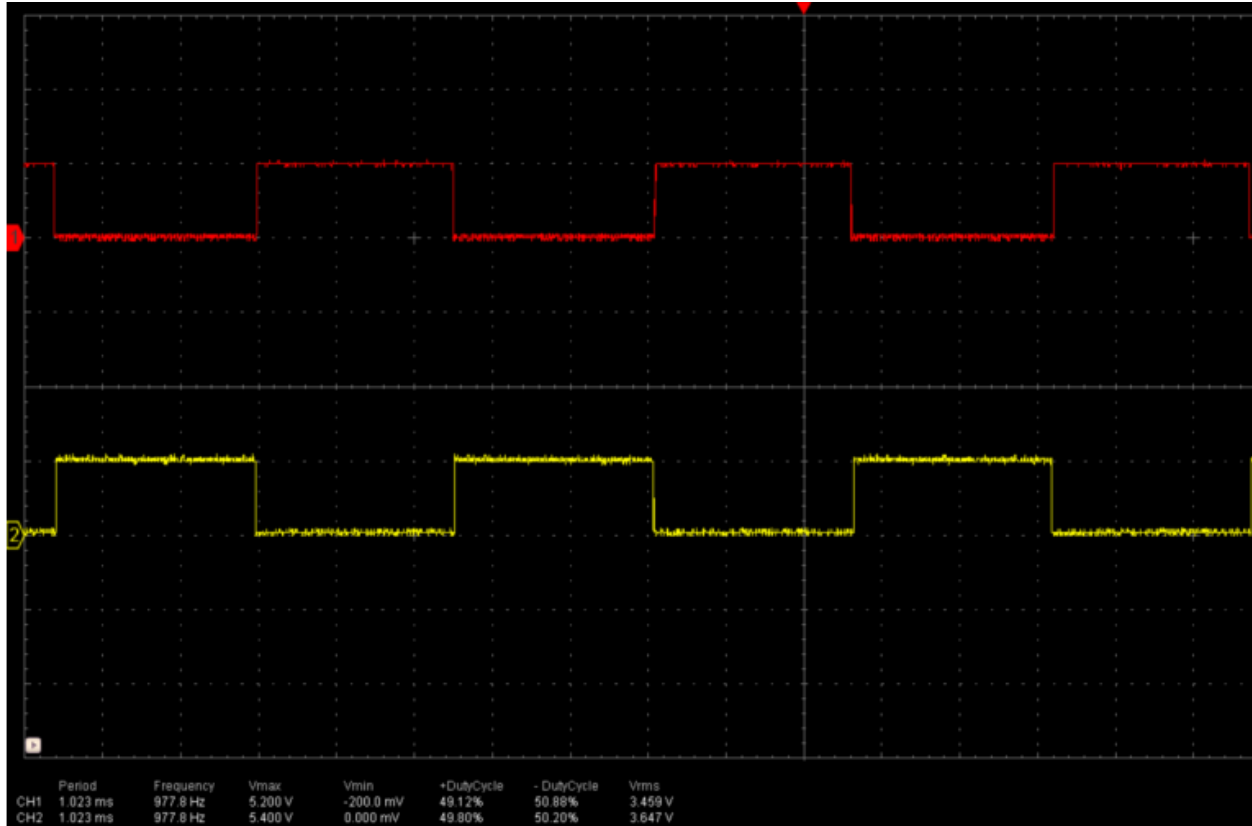


Figure 37: Measured Control Waveforms.

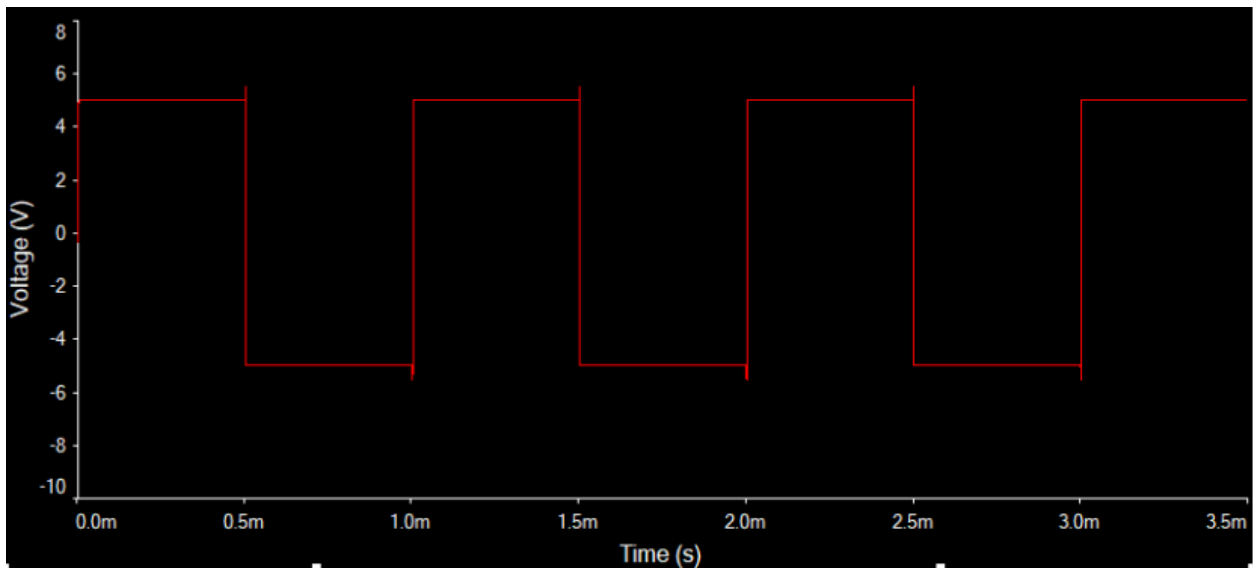
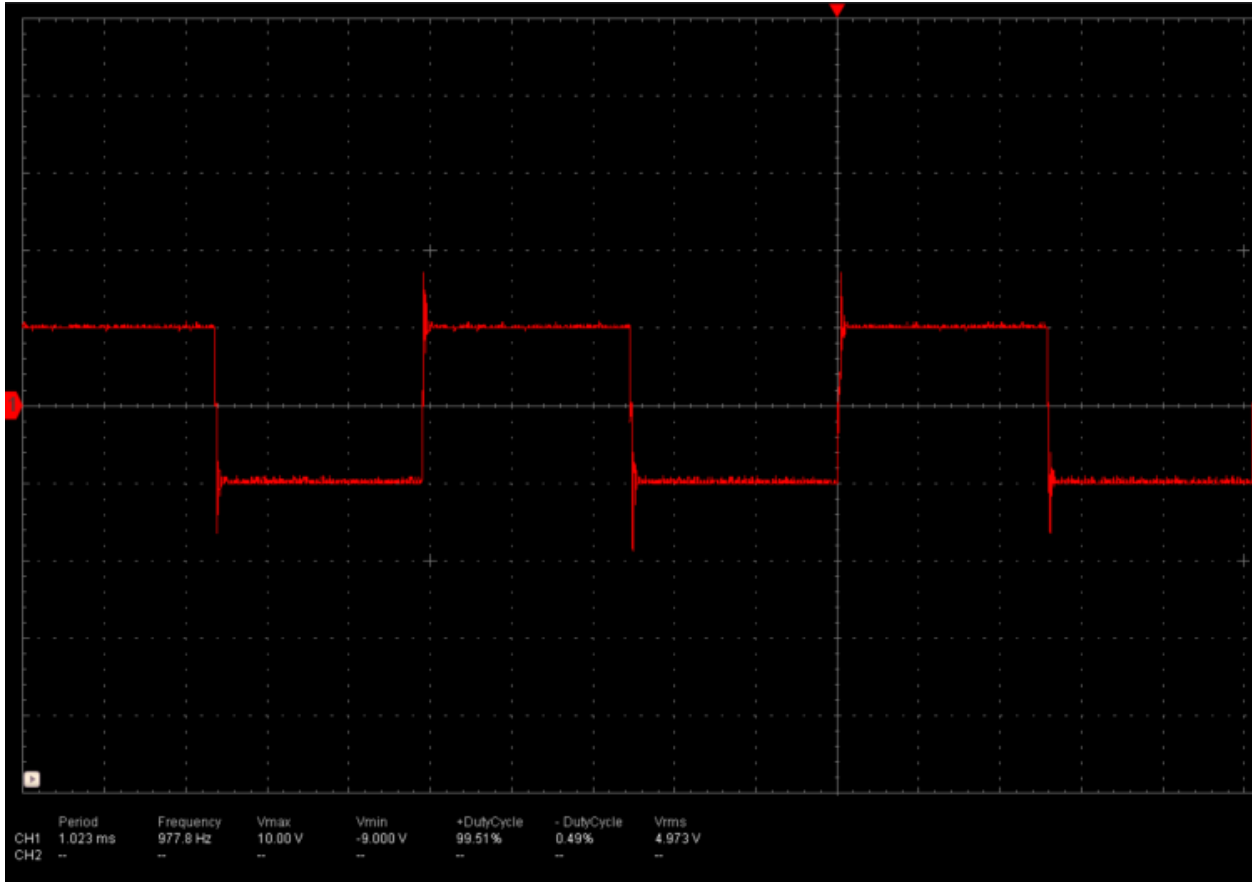
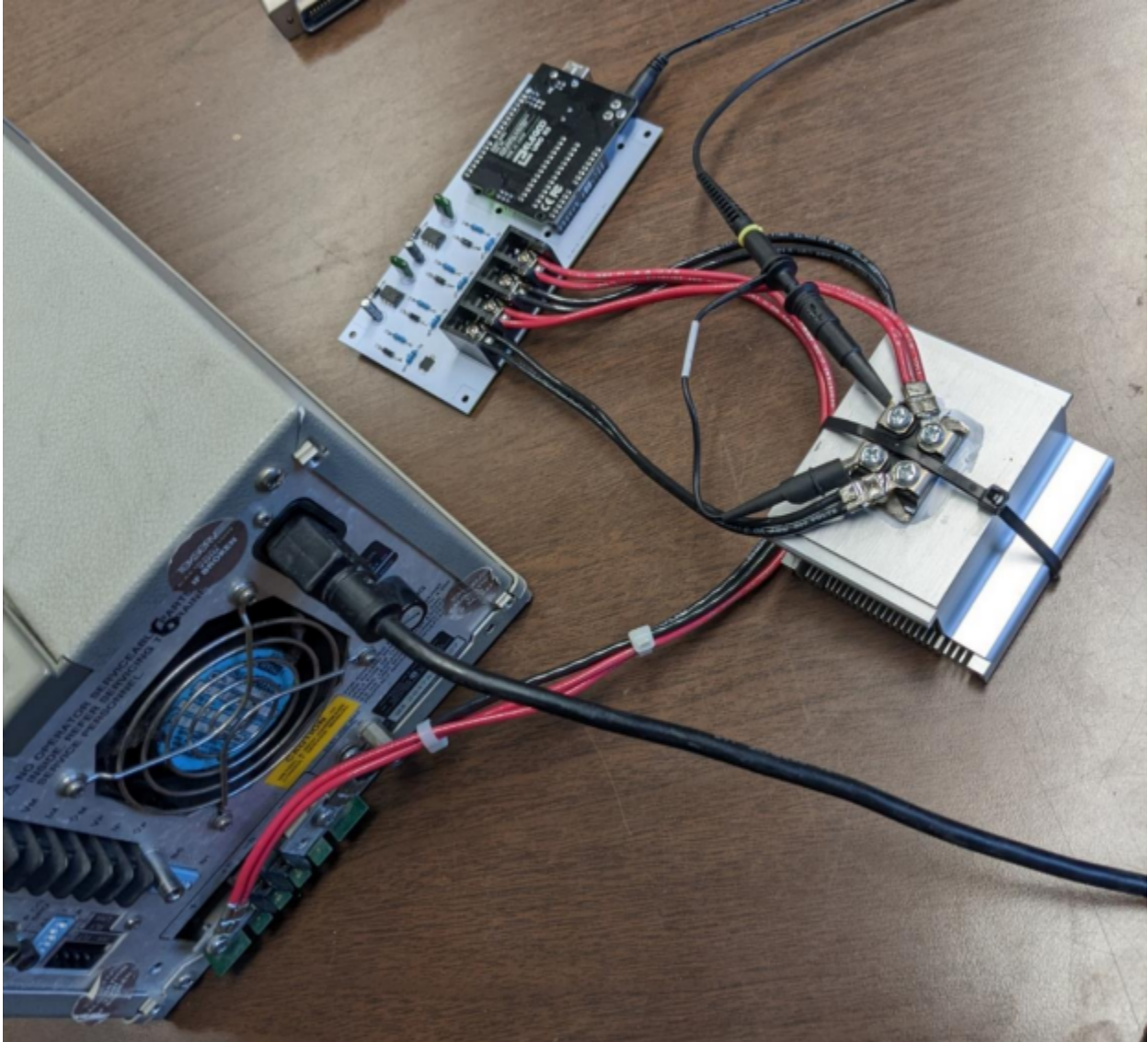


Figure 38: Simulated Output Waveform.



*Figure 39: Measured Output Waveform.*

### Thermal Performance Test



*Figure 40: High Current Behavior Testing.*

From our testing, we found the ideal operating range for the switch to be currents less than 15A. Although the switch was able to handle currents up to 22A, currents beyond the 15A threshold caused the MOSFETs to become “too hot to touch.” High temperatures can accelerate the degradation of the MOSFETs, shortening their life and increasing the risk of thermal runaway. Although the MOSFETs temperature rise was accounted for and predicted, the actual temperature rise far exceeded our expectations. This could be explained by unaccounted sources of heat, such as power dissipation in the PCB’s traces.

## Chapter 4: Impacts

### 4.1 Engineering Ethics

The code of ethics of engineers is a vital set of principles that engineers must follow when conducting their work. As engineers, we emphasized the importance of following these three principles while working on this project. The first is to use our knowledge and skills to enhance human welfare. The work we conducted on this project is part of a larger initiative to improve and scale a new method to make solar silicon. The advantages of this process are that it's both economical and less impactful on the environment than current manufacturing methods. Making solar silicon cheaper to produce allows for solar panels to be more affordable for consumers who could typically not afford them. The life cycle analysis that was performed was to estimate the environmental impact of this process where it was concluded that it is far less impactful than current methods. The experimental augmentation component of the project worked on improvements to the process to move it closer to a baseline using a switch and silicon nitride coating. Continued work on the electrolysis method that has both of these advantages can assist the globe in combating climate change which puts all of humanity at risk.

The second fundamental principle of engineers is to be honest and impartial about the work they conduct. For the life cycle analysis component of the project, it was important that the scope and goals of the assessment are clearly indicated. This helps to provide necessary context to those who review the results in the future. In addition, there were elements to the LCA that could not be included due to lack of technical information on some processes. These limitations as well as any assumptions that were made along the way are clearly stated in the report to ensure that we are honest with our assessment.

The last fundamental principle of engineers is to strive to increase the competence and prestige of the engineering profession. As a group, we were all very passionate about this project and wanted to ensure that we contributed high-quality work to assist this process in the future. The members of this group are from various engineering departments and each contributed to the areas of this project that they are competent. With the knowledge attributed from our study and the assistance of our advisors, we were able to successfully conduct a life cycle assessment, an electrical switch, and an analysis of the silicon nitride coating. The hope of this group is that the



findings from this project will be used and improved upon by future groups to continue to enhance the solar silicon electrolysis process.

#### **4.2 Societal and Global Impacts**

This project has the potential to impact both individuals as well as the global silicon industry. While the specifics of the work center around a comprehensive life cycle analysis and experimental augmentations, the new process which they support promises to produce high purity silicon for a much lesser cost than that of current methods. A significant reduction in the price of silicon would have profound impacts on the many industries which utilize the material, including the automotive, battery, and solar industries. In the case of solar, the reduction in price would help accelerate the world's transition to renewable energy, as solar panels would be cheaper to produce and overall more available to consumers. Additionally, the reduction in cost could help developing countries construct more robust power infrastructure. Unlike other forms of power generation which require complex and costly machinery, solar panels are relatively cheap, require much less maintenance, and are easier to implement. The increased availability of power would promote general welfare as people in the affected communities would gain access to the many luxuries of modern life which require power.

#### **4.3 Environmental Impact**

From the life cycle analysis that was conducted, environmental impacts of molten salt electrolysis can be directly observed. Most of the environmental impacts of this production method comes from prior mining and refinement for a variety of salt bath components, silicon dioxide, as well as fuel for transportation. Ecotoxicity in freshwater is one impact that was larger than most of the categories analyzed. Ecotoxicity is a reference to potential chemical, biological, or physical stressors to affect ecosystems. This analysis equates ecotoxicity values to that of 1, 4 dichlorobenzene in order to have a measurable effect on surrounding ecosystems. Increases in mining and refinement can lead to a higher ecotoxicity impact in turn leading to a possible compromise of the local ecosystem. This disruption can cause bioaccumulation in both freshwater species as well as humans who may be living in areas nearby these mines.

Another impact for this analysis includes climate change categories. These impacts were equated by using carbon dioxide values. Carbon dioxide has been shown to directly increase global average temperatures due to the fact that carbon dioxide is a greenhouse gas, allowing heat to be trapped more easily in the atmosphere. This new process being proposed has shown potential for producing less climate change than that of the Siemens process when comparing carbon dioxide emissions of the two processes.

Overall, we see a trend in a gate to gate comparison of the Siemens process to that of the electrolysis process. The Siemens process had a much higher total environmental impact than that of the electrolysis process. In turn, this newly proposed method would lead to lower effects to human health and the environment overall.

#### **4.4 Codes and Standards**

For the creation of the life cycle analysis, there were codes that needed to be followed such that the life cycle analysis would be effective. These are the ISO standards, discussed at the beginning at chapter 2. These standards served as a guideline for this project to ensure that the results gathered were as accurate and useful as possible so that they can potentially have application in the real world.

#### **4.5 Economic Factors**

From the large variety of work that was done, through the simulations of the life cycle analysis and the experimental augmentations done, there has been much progress in getting the molten salt electrolysis process closer to being a commercial process. Starting with the life cycle analysis, the process of a potential scale up was analyzed such that as the business side of the process begins to expand, there is a much better understanding of potential locations for not only the electrolysis process itself, but also the raw materials needed for the process. This allows any company that intends to run a business around this process to know both where they could potentially get every material, but also how each of these materials will be transported, jumpstarting the entire process.

On the experimental side, the creation of the switch for creating oscillating current is the next step in making the electrolysis process commercial. A mass producible version of this switch will be necessary in the long term so its creation here is an important first step. As the lab work continues, a baseline will eventually be achieved with a high enough concentration of silica to be used leading to a better future for the molten salt electrolysis process, and a better, more efficient future for the creation of solar silicon. The silicon nitride coating prolonged the electrolysis process and guaranteed a steadier yield of silicon, reaching a step closer to commercialization.

## **Chapter 5: Conclusion**

### **5.1 Life Cycle Analysis**

The life cycle analysis was created for its ability to accurately simulate environmental impacts related to the production of solar silicon for solar panels. This simulation utilized the most up to date material balance as well as supplementary life cycle analyses for environmental calculations. From this life cycle analysis it was discovered that  $MgF_2$  had the largest environmental impact out of all salt bath components, having the highest contribution in 16 out of the 19 impact categories, mining and refinement was the largest contribution group, having 17 out of the 19 largest impacts in all impact categories, and in a comparison of the gate to gate production of solar grade silicon using molten electrolysis or the Siemens process, it was found that molten electrolysis had a significantly smaller impact than that of the Siemens process.

### **5.2 Experimental Component**

The silicon nitride coating showed greater resistance to oxygenated corrosion on the coated silicon wafer relative to the silicon wafer without a coating. More experiments with a coated wafer will need to be done to affirm lesser shrinking on the silicon wafer.

### **5.3 Electrical Switch**

From our data, it appears the lab-scale switch works as intended, producing the desired output pulses across various load and power configurations. However, in its current configuration the current range must be limited so as not to exceed the limits of the desired operating temperature range. Further work could address these performance concerns by implementing additional heat management protocols for the MOSFETs. This could take the form of a redesigned PCB Board with added area for board mounted heat sinks or reusing the board and porting the MOSFET connections out to an external MOSFET array mounted on a heatsink, similar in form to the load used in high current testing (see Appendix A).

## Chapter 6: Bibliography

- An, J., & Xue, X. (2017). Life-cycle carbon footprint analysis of magnesia products. *Resources, Conservation and Recycling*, 119, 4-11. doi:10.1016/j.resconrec.2016.09.023
- Aulich, H.A., Eisenrith, K.H. & Urbach, H.P. New methods to prepare high-purity silica. *J Mater Sci* 19, 1710–1717 (1984). <https://doi.org/10.1007/BF00563069>
- Chandrasekar, M.S., & Pushpavanam, M. (2008, March 10). Pulse and pulse reverse plating—Conceptual, advantages and applications. *Electrochimica Acta*, 53(8), 3313-3322. Science Direct. <https://doi.org/10.1016/j.electacta.2007.11.054>.
- Chester, M. (n.d.). Transportation LCA: Freight Database. Transportation LCA | Freight Database. Retrieved November 19, 2021, from <http://www.transportationlca.org/tlcadb-freight.php>.
- Corathers, L. A., Pizzini, S., Calligarich, S. P., Calligarich, Barron, C. S., Smith, C., & Barron. (n.d.). Refining Silicon. Retrieved from <https://www.pveducation.org/pvcdrom/manufacturing-si-cells/refining-silicon>
- Egilmez, G., & Park, Y. S. (2014). Transportation related carbon, energy and water footprint analysis of U.S. manufacturing: An eco-efficiency assessment. *Transportation Research Part D: Transport and Environment*, 32, 143–159. <https://doi.org/10.1016/j.trd.2014.07.001>
- Facanha, C. (n.d.). Evaluation of Life-Cycle Air Emission Factors of Freight Transportation. Retrieved November 19, 2021, from <https://pubs.acs.org/doi/pdf/10.1021/es070989q>.
- Gerberding, J. L. (2003). Toxicological Profile For Fluorides, Hydrogen Fluoride, And Fluorine. Report prepared for the U.S. Department Of Health And Human Services. Public Health Service. Washington.
- Goodin, R. C. (n.d.). National Minerals Information Center. Retrieved October 23, 2021, from <https://www.usgs.gov/centers/nmic/silica-statistics-and-information>
- Goods Movement Life Cycle Assessment for Greenhouse Gas Reduction Goals. (n.d.). Retrieved November 19, 2021, from <https://onlinelibrary.wiley.com/doi/epdf/10.1111/jiec.12277>.
- Grbeš, A. (2015). A Life Cycle Assessment of Silica Sand: Comparing the Beneficiation

Processes. *Sustainability*, 8(1), 11. doi:10.3390/su8010011

How Lime is Made. (n.d.). Retrieved from <https://www.lime.org/lime-basics/how-lime-is-made/>

How Quartz Is Processed For Use In Everyday Products. (2021, October 23). Retrieved from <https://www.mclanahan.com/blog/how-quartz-is-processed-for-use-in-everyday-products>

Joseph, A., Kirubasankar, B., Matthew, A. M., Narayanasamy, M., Yan, C., & Angaiah, S. (2021, September 1). Influence of pulse reverse current parameters on electrodeposition of copper-graphene nanocomposite coating. *Applied Surface Science Advances*, 5(2021). Science Direct. <https://doi.org/10.1016/j.apsadv.2021.100116>.

Khoo, H. H., Bu, J., Wong, R. L., Kuan, S. Y., & Sharratt, P. N. (2011). Carbon capture and utilization: Preliminary life cycle CO<sub>2</sub>, energy, and cost results of potential mineral carbonation. *Energy Procedia*, 4, 2494–2501. <https://doi.org/10.1016/j.egypro.2011.02.145>

Koltun, P., & Tharumarajah, A. (2014). Life cycle impact of rare earth elements. *ISRN Metallurgy*, 2014, 1–10. <https://doi.org/10.1155/2014/907536>

Li, J., Zhang, Y., Shao, S., & Zhang, S. (2015). Comparative life cycle assessment of conventional and new fused magnesia production. *Journal of Cleaner Production*, 91, 170-179. doi:10.1016/j.jclepro.2014.12.043

Lovett, R. A. (2002, June 12). Global Warming Tied to Ozone Recovery. *Science*. Retrieved March 24, 2022, from <https://www.science.org/content/article/global-warming-tied-ozone-recovery#:~:text=In%20the%20harsh%20sunlight%20of,other%20chemicals%20that%20destroy%20ozone.>

Manfredi, S., Allacker, K., Chomkamsri, K., Pelletier, N., & de Souza, D. M. (2012, July 17). PEF methodology final draft. Ispra, Italy; European Commission-Joint Research Centre.

Marinshaw, R. et al. (1994). *Emission Factor Documentation for AP-42: Lime Manufacturing*. Report prepared for U.S. Environmental Protection Agency. Washington.

Moudgal, A., Buasai, S., Wu, Y. J., McMahan, A., Hazerjian, J. M., Luu, V., Ly, A., Asadikiya, M., Powell, A. C., Pal, U., & Zhong, Y. (2020, December 18). Finite Element Analysis and Techno-economic Modeling of Solar Silicon Molten Salt Electrolysis. *JOM*, 73, 233-243. <https://doi.org/10.1007/s11837-020-04468-y>

Navarro, J., & Zhao, F. (2014). Life-Cycle Assessment of the Production of Rare-Earth Elements for Energy Applications: A Review. *Frontiers in Energy Research*, 2, 45.

doi:10.3389/fenrg.2014.00045

- Osipova, M.L., Murashova, I.B., & Savel'ev, A.M. (2010, October 30). Formation of dendritic copper deposit in industrial electrolysis. *Powder Metall Met Ceram*, 49, 253-259.  
<https://doi.org/10.1007/s11106-010-9230-8>
- Portmann, R. W., Daniel, J. S., & Ravishankara, A. R. (2012). Stratospheric ozone depletion due to nitrous oxide: Influences of other gasses. *Philosophical Transactions of the Royal Society B: Biological Sciences*, 367(1593), 1256–1264.  
<https://doi.org/10.1098/rstb.2011.0377>
- Prioleau, T. K. (2003). (working paper). *Environmental Impact of the Petroleum Industry*. Hazardous Substance Research Centers/South & Southwest Outreach Program. Retrieved March 23, 2022, from  
[https://cfpub.epa.gov/ncer\\_abstracts/index.cfm/fuseaction/display.files/fileID/1452](https://cfpub.epa.gov/ncer_abstracts/index.cfm/fuseaction/display.files/fileID/1452).
- Ropp, R. C. (2013). *Encyclopedia of the alkaline earth compounds*. Kidlington, Oxford.  
doi:<https://doi.org/10.1016/B978-0-444-59550-8.00002-8>.
- Steinmann, Z., & Huijbregts, M. A. J. (n.d.). (rep.). *Stratospheric ozone depletion*. LC-Impact. Retrieved March 23, 2022, from  
[https://lc-impact.eu/doc/method/Chapter3\\_Stratospheric-ozone-depletion.pdf](https://lc-impact.eu/doc/method/Chapter3_Stratospheric-ozone-depletion.pdf).
- Stodolsky, F.; Gaines, L.; Cuenca, R.; Eberhardt, J. Lifecycle analysis for freight transport. Paper no. 982206 in Proceedings of the 1998 Total Life-cycle Conference; Society of Automotive Engineers, Inc.: Warrendale, PA, 1998.
- Taşçioğlu, A., Taşkın, O., & Vardar, A. (2016). A power case study for monocrystalline and polycrystalline solar panels in Bursa City, Turkey. *International Journal of Photoenergy*, 2016, 1–7. <https://doi.org/10.1155/2016/7324138>
- Torgal, F. P., Shi, C., & Sánchez, A. P. (2018). *Carbon Dioxide Sequestration in Cementitious Construction Materials*. Woodhead Publishing.  
doi:<https://doi.org/10.1016/B978-0-08-102444-7.09001-8>.
- U.S. Environmental Protection Agency. (April, 2021). *U.S. Greenhouse Gas Emissions and Sinks* (Report No. 430-R-21-005). Retrieved from  
<https://www.epa.gov/ghgemissions/inventory-us-greenhouse-gas-emissions-and-sinks-1990-2019>

What is Lime: Lime vs Limestone. (2021, October 08). Retrieved from

<https://mintekresources.com/what-is-lime/>

*What are the units of characterization factors in USEtox?* USEtox®. (2022). Retrieved March 31, 2022, from <https://www.usetox.org/faq-page/23-0#t23n78>

Wiechmann, E., Aqueveque, P., & Morales, A. S. (2010, September). Improving Productivity and Energy Efficiency in Copper Electrowinning Plants. *IEEE Transactions on Industry Applications*, 46(4), 1264-1270. Research Gate. 10.1109/TIA.2010.2049818

Wills, B. A., & Finch, J. A. (2016). *Wills Mineral Processing Technology (Eighth Edition)* (8th ed.). Butterworth-Heinemann. doi:<https://doi.org/10.1016/B978-0-08-097053-0.00010-8>.

Wuebbles, D. J., & Tamareisis, J. S. (1993). The role of methane in the global environment. *Atmospheric Methane: Sources, Sinks, and Role in Global Change*, 469–513. [https://doi.org/10.1007/978-3-642-84605-2\\_20](https://doi.org/10.1007/978-3-642-84605-2_20)

Xu, Y., Li, J., Tan, Q., Peters, A. L., & Yang, C. (2018). Global status of Recycling Waste Solar Panels: A Review. *Waste Management*, 75, 450–458. <https://doi.org/10.1016/j.wasman.2018.01.036>

Yttrium. (n.d.). Retrieved from <https://www.britannica.com/science/yttrium>

Yttrium. (n.d.). Retrieved from <https://mineralseducationcoalition.org/elements/yttrium/>

YTTRIUM FLUORIDE PROCESSES. (n.d.). Retrieved from

<https://materion.com/resource-center/newsletters/coating-materials-news/yttrium-fluoride-processes>

Zhang, C., Sun, W., Hu, Y., Tang, H., Yin, Z., Guan, Q., & Gao, J. (2018). Investigation of two-stage depressing by using hydrophilic polymer to improve the process of fluorite flotation. *Journal of Cleaner Production*, 193, 228-235. doi:10.1016/j.jclepro.2018.05.055

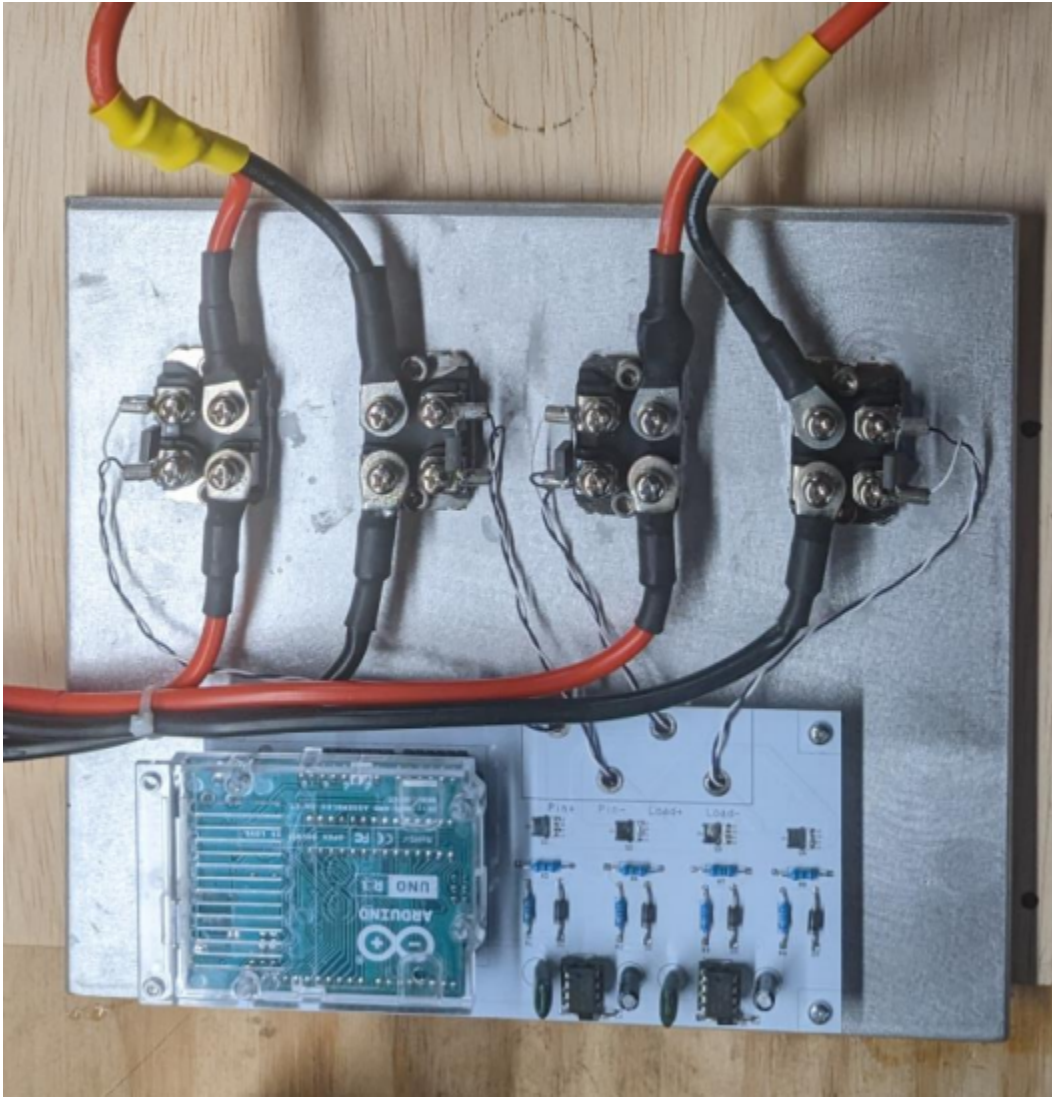
International Organization for Standardization. (2016). *Occupational health and safety management systems—Requirements with guidance for use* (ISO/DIS Standard No. 45001). Retrieved from [http://www.iso.org/iso/catalogue\\_detail?csnumber=63787](http://www.iso.org/iso/catalogue_detail?csnumber=63787)

(International Organization for Standardization [ISO], 2016)



U.S. Environmental Protection Agency. (1990-2019). *U.S. Greenhouse Gas Emissions and Sinks* (Report No. 430-R-21-005). Retrieved from <https://www.epa.gov/ghgemissions/inventory-us-greenhouse-gas-emissions-and-sinks-1990-2019>

## Appendix A



Redesigned Cell Driver with improved heat management